

1-2019

## Alkalinity in Tidal Tributaries of the Chesapeake Bay

R. G. Najjar

M. Herrmann

S. M. Cintrón Del Valle

Jaclyn R. Friedman

*Virginia Institute of Marine Science*

Marjorie A.M. Friedrichs

*Virginia Institute of Marine Science**See next page for additional authors*Follow this and additional works at: <https://scholarworks.wm.edu/vimsarticles>Part of the [Marine Biology Commons](#), and the [Oceanography Commons](#)

---

### Recommended Citation

Najjar, R. G.; Herrmann, M.; Cintrón Del Valle, S. M.; Friedman, Jaclyn R.; Friedrichs, Marjorie A.M.; and et al, Alkalinity in Tidal Tributaries of the Chesapeake Bay (2019). *JGR Oceans*, 125(1), e2019JC015597. doi:10.1029/2019JC015597

This Article is brought to you for free and open access by the Virginia Institute of Marine Science at W&M ScholarWorks. It has been accepted for inclusion in VIMS Articles by an authorized administrator of W&M ScholarWorks. For more information, please contact [scholarworks@wm.edu](mailto:scholarworks@wm.edu).

---

**Authors**

R. G. Najjar, M. Herrmann, S. M. Cintrón Del Valle, Jaclyn R. Friedman, Marjorie A.M. Friedrichs, and et al

## RESEARCH ARTICLE

10.1029/2019JC015597

## Special Section:

Carbon cycling in tidal wetlands and estuaries of the contiguous United States

## Key Points:

- The long-term means of alkalinity in fresh waters of the Chesapeake Bay vary by a factor of 6 among seven tidal tributaries
- Tidal tributaries fed by high-alkalinity rivers have alkalinity sinks and those fed by low-alkalinity rivers have alkalinity sources
- The alkalinity sink in the Potomac River Estuary declined from 1986 to 2013, leading alkalinity to increase in this system

## Supporting Information:

- Supporting Information S1

## Correspondence to:

R. G. Najjar,  
rgn1@psu.edu

## Citation:








Najjar, R. G., Herrmann, M., Cintrón Del Valle, S. M., Friedman, J. R., Friedrichs, M. A. M., Harris, L. A., et al. (2020). Alkalinity in tidal tributaries of the Chesapeake Bay. *Journal of Geophysical Research: Oceans*, 125, e2019JC015597. <https://doi.org/10.1029/2019JC015597>

Received 25 AUG 2019

Accepted 18 NOV 2019

Accepted article online 10 DEC 2019

## Alkalinity in Tidal Tributaries of the Chesapeake Bay

Raymond G. Najjar<sup>1</sup> , Maria Herrmann<sup>1</sup>, Sebastián M. Cintrón Del Valle<sup>2</sup>, Jaclyn R. Friedman<sup>3</sup> , Marjorie A.M. Friedrichs<sup>3</sup> , Lora A. Harris<sup>4</sup> , Elizabeth H. Shadwick<sup>5</sup> , Edward G. Stets<sup>6</sup> , and Ryan J. Woodland<sup>4</sup> 

<sup>1</sup>Department of Meteorology and Atmospheric Science, The Pennsylvania State University, University Park, PA, USA,<sup>2</sup>Physics Department, University of Puerto Rico, Mayagüez Campus, Mayagüez, Puerto Rico, <sup>3</sup>Virginia Institute of Marine Science, William & Mary, Gloucester Point, VA, USA, <sup>4</sup>Chesapeake Biological Laboratory, University of Maryland Center for Environmental Science, Solomons, MD, USA, <sup>5</sup>CSIRO, Oceans & Atmosphere, Hobart, TAS, Australia, <sup>6</sup>United States Geological Survey, Mounds View, MN, USA

**Abstract** Despite the important role of alkalinity in estuarine carbon cycling, the seasonal and decadal variability of alkalinity, particularly within multiple tidal tributaries of the same estuary, is poorly understood. Here we analyze more than 25,000 alkalinity measurements, mostly from the 1980s and 1990s, in the major tidal tributaries of the Chesapeake Bay, a large, coastal-plain estuary of eastern North America. The long-term means of alkalinity in tidal-fresh waters vary by a factor of 6 among seven tidal tributaries, reflecting the alkalinity of nontidal rivers draining to these estuaries. At 25 stations, mostly in the Potomac River Estuary, we find significant long-term increasing trends that exceed the trends in the nontidal rivers upstream of those stations. Box model calculations in the Potomac River Estuary indicate that the main cause of the estuarine trends is a declining alkalinity sink. The magnitude of this sink is consistent with a simple model of calcification by the invasive bivalve *Corbicula fluminea*. More generally, in tidal tributaries fed by high-alkalinity nontidal rivers, alkalinity is consumed, with sinks ranging from 8% to 27% of the upstream input. In contrast, tidal tributaries that are fed by low-alkalinity nontidal rivers have sources of alkalinity amounting to 34% to 171% of the upstream input. For a single estuarine system, the Chesapeake Bay has diverse alkalinity dynamics and can thus serve as a laboratory for studying the numerous processes influencing alkalinity among the world's estuaries.

**Plain Language Summary** Alkalinity, which is the capacity of a water body to neutralize acid, is a useful quantity when studying the cycling of carbon in water bodies, including estuaries. Here we analyze alkalinity measurements in tidal tributaries of the Chesapeake Bay. Average alkalinity levels in the freshest parts of the estuaries varied by sixfold among seven tidal tributaries. Alkalinity was also found to increase over several decades at several locations, partially due to alkalinity increases in the rivers draining to Chesapeake Bay and also probably due to a reduction in the processes that remove alkalinity from estuarine waters. Evidence also supports the role of an invasive species, the Asiatic Clam, in the alkalinity removal in the Potomac River Estuary. More generally, we found evidence that tidal tributaries fed by high-alkalinity rivers consumed alkalinity while tidal tributaries that are fed by low-alkalinity rivers produce alkalinity. For a single estuarine system, the Chesapeake Bay has a wide range of alkalinity levels and a wide variety of processes that influence its alkalinity. Therefore, the Chesapeake Bay can serve as a laboratory for studying the alkalinity of many of the world's estuaries.

## 1. Introduction

Carbon is a currency for quantifying important features of estuaries, such as their support of high biological productivity and their role in linking the biogeochemical cycles of the land and sea. Central to understanding controls on carbon is the total or titration alkalinity (hereafter “alkalinity”), which plays a prominent role in determining the partitioning of dissolved inorganic carbon among carbon dioxide, carbonate ion, and bicarbonate ion, and thus influences key estuarine processes, such as air–water exchange of carbon dioxide and changing pH due to eutrophication and uptake of anthropogenic CO<sub>2</sub> (Cai et al., 2011; Carstensen & Duarte, 2019).

There is some evidence that alkalinity is changing in estuaries (Carstensen et al., 2018; Gustafsson et al., 2019; Hu et al., 2015; Müller et al., 2016; Prasad et al., 2013). Because of the important role of

conservative mixing between marine and freshwater endmembers in controlling the alkalinity distribution (Brust & Newcombe, 1940; Carpenter et al., 1975; Cifuentes et al., 1990; Mook & Koene, 1975; Park et al., 1971; Pelletier & Lebel, 1979; Turekian, 1971; Wong, 1979), long-term trends in watershed alkalinity (Carstensen et al., 2018; Drake et al., 2018; Kaushal et al., 2013; Raymond et al., 2008; Raymond & Oh, 2009; Stets et al., 2014) must be having some influence on estuarine alkalinity. Additionally, non-conservative behavior due to biogeochemical transformations involving sulfur (Cai et al., 2017; Raymond et al., 2000; Smith & Hollibaugh, 1997; Yao & Millero, 1995), calcium (Hu et al., 2015; Liu et al., 2014; Manickam et al., 1985; Wartel & Faas, 1986), and nitrogen (Abril & Frankignoulle, 2001; Dai et al., 2006; Frankignoulle et al., 1996), or a combination of these factors (Abril et al., 1999; Cai et al., 2017; Cai & Wang, 1998; Carstensen et al., 2018; Cerco et al., 2013) has been identified. However, fewer studies have quantified rates of alkalinity consumption or production within estuaries (Brodeur et al., 2019; Cai & Wang, 1998; Cerco et al., 2013; Joesoef et al., 2017; Raymond et al., 2000; Smith & Hollibaugh, 1997; Wang & Cai, 2004) and we are unaware of any studies that have examined seasonal and decadal variability of alkalinity across multiple tidal tributaries of the same estuary.

This study is focused on the alkalinity distribution in the Chesapeake Bay, providing an analysis of more than 25,000 alkalinity observations made by the Chesapeake Bay Program between 1984 and 2018 in the bay's major tidal tributaries. Despite the Chesapeake Bay being one of the most intensively monitored estuaries in the world, there were, until recently (Brodeur et al., 2019; Cai et al., 2017; Shadwick et al., 2019; Shen et al., 2019), relatively few studies of its alkalinity distribution, most of which were focused on a single tidal tributary of the bay (Brust & Newcombe, 1940; Carpenter et al., 1975; Cerco et al., 2013; Wong, 1979). Early work pointed out the relationship between alkalinity and salinity, with studies of low-salinity waters noting a nonzero fresh water endmember (Brust & Newcombe, 1940) that varies seasonally and interannually (Carpenter et al., 1975), and studies of high-salinity waters noting conservative mixing but also recognizing the possibility of biogeochemical sources and sinks (Bates & Hansell, 1999; Wong, 1979). The emphasis of more recent work has been on quantifying these sources and sinks. Cerco et al. (2013) modeled alkalinity in the tidal-fresh portion of the Potomac River Estuary, finding that 16% of the alkalinity load from the watershed was consumed under average hydrological conditions through a variety of processes. Recent observational (Brodeur et al., 2019; Cai et al., 2017) and modeling (Shen et al., 2019) studies in the mainstem bay have emphasized  $\text{CaCO}_3$  precipitation at low salinities, perhaps in association with seagrasses, and dissolution in subsurface waters at high salinity.

Waldbusser et al. (2013) analyzed nearly 10,000 observations of alkalinity made by the Chesapeake Bay Program throughout the estuary, mostly from low-salinity regions. Alkalinity was found to increase quadratically with salinity and with a positive second derivative; the authors inferred that the bay as a whole is a sink of alkalinity, possibly due to bivalve calcification. Furthermore, Waldbusser et al. (2013) found variability in alkalinity to increase at low salinities, which suggests multiple freshwater endmembers, temporal variability in the freshwater endmember, or both. Several other studies have indicated strong evidence for decadal-scale increases in the alkalinity of rivers draining to the Chesapeake Bay (Kaushal et al., 2013; Raymond & Oh, 2009; Stets et al., 2014), although no studies have been conducted to determine whether a signal of these increases is present anywhere in the estuary. In summary, while the understanding of the temporal and spatial dynamics of alkalinity in Chesapeake Bay and the rivers that feed it has improved in recent years, a comprehensive analysis of Chesapeake Bay Program alkalinity data set offers an important opportunity to provide insights into the rates and processes that affect alkalinity dynamics in a diverse and complex estuary. The diversity of environments in a single system also offers an opportunity to reach conclusions that may hold for other systems as well.

In this study, we document the variability of alkalinity in Chesapeake Bay, with a focus on the major tidal tributaries (or subestuaries), where most of the measurements were made. We describe seasonal and interannual variability as well as the differences among the tidal tributaries and the variability along the main axis of each tidal tributary. To understand this variability, an analysis is first presented of the alkalinity just above the head of tide of rivers entering the Chesapeake Bay. To quantify sources and sinks of alkalinity in the tidal tributaries, a standard steady-state mixing-model approach is adopted (Boyle et al., 1974). A more in-depth analysis of the alkalinity budget is provided by applying a box model to the Potomac River Estuary, where data coverage in space and time is excellent. To provide an ecological context for the alkalinity budget of the Potomac River Estuary, data on seagrasses and bivalves are analyzed.

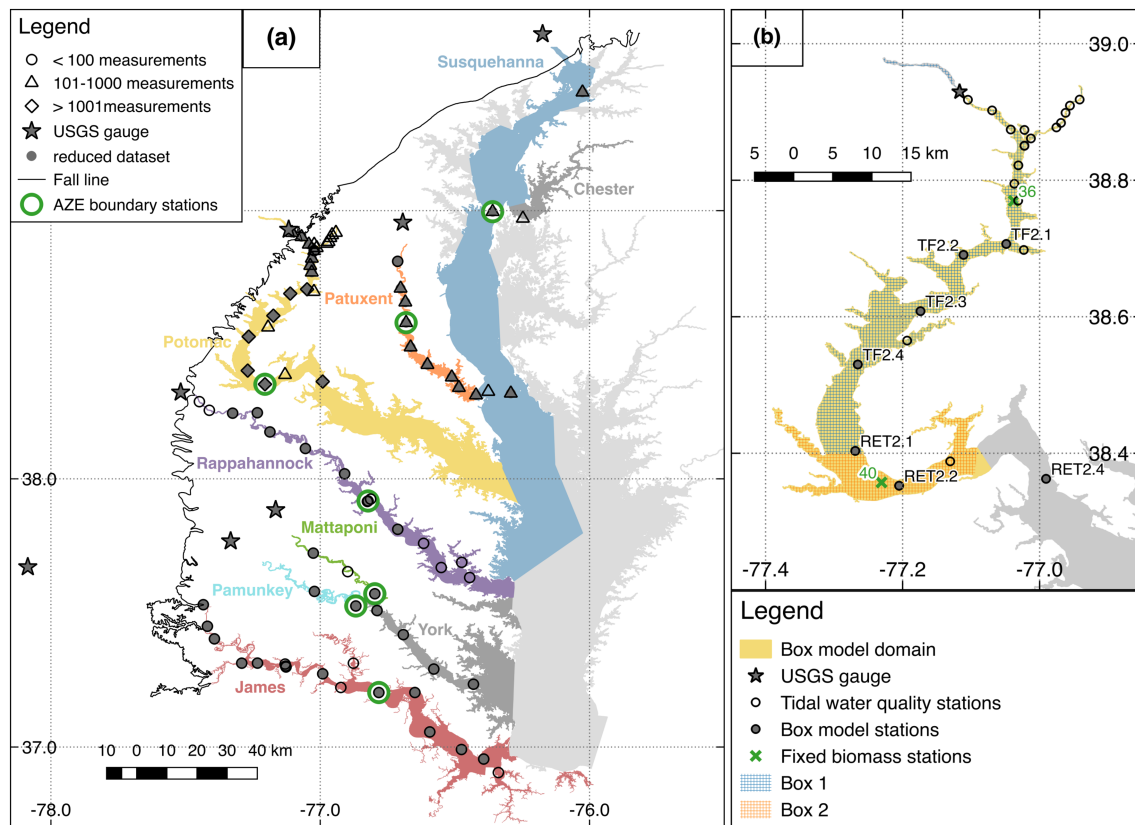


**Figure 1.** (a) Location of alkalinity measurements in the tidal tributaries and at the river gauges. Number of measurements is indicated, as are boundary stations for the apparent zero-salinity endmember (AZE) model. (b) Enlarged view of the upstream portion of the Potomac River Estuary, showing stations with long-term alkalinity data sets, stations used in the box-model calculation, and the box-model domain. Fixed sampling stations of bivalve biomass are shown (36 and 40) as well as boundaries over which bivalve biomass from random sampling and submerged aquatic vegetation coverage was computed: Box 1 (tidal fresh) and Box 2 (oligohaline).

## 2. Data and Methods

### 2.1. Water Chemistry Data in the Tidal Tributaries

The alkalinity data set analyzed here comes from the Chesapeake Bay Program's Water Quality Database. Preliminary processing of the data followed these steps: (1) removal of outliers, (2) removal of alkalinity measurements that did not have a corresponding known value of salinity, and (3) removal of stations that contained very few measurements. Details are provided in supporting information Text S1 and Table S1. This processing reduced the alkalinity data set to 25,289 measurements across 80 stations ("whole processed data set," hereafter).

To analyze the spatial variability of alkalinity, the bay was separated into seven tidal tributaries (Figure 1a and Tables S1 and S2), based on the standard management segmentation scheme developed by the Chesapeake Bay Program (2004): the Susquehanna River Estuary, the Patuxent River Estuary, the Potomac River Estuary, the Rappahannock River Estuary, the York River Estuary, the James River Estuary, and the Chester River Estuary. In some analyses, the upper York River Estuary was split into two tidal tributaries, the Mattaponi and Pamunkey River Estuaries, reflecting the two main sources of fresh water to the York River Estuary.

Data coverage is uneven in space and time. The Potomac River Estuary stands out as the only tidal tributary that was monitored after 2005 and as the tidal tributary that contains the most observations and stations, 70% and 31% of the respective totals (Table S1). Measurements in the Susquehanna and Patuxent River Estuaries are mainly from the late 1980s while the monitoring in the other estuaries (except the Potomac River

Estuary) is limited to the 1990s (Table S1). Whereas the Patuxent, Rappahannock, York, and James River Estuaries have good horizontal coverage, there are no data in the downstream half of the Potomac River Estuary, and there is only one station in the Chester River Estuary (Figure 1a). Data are essentially confined to the surface (<5 m) for the Rappahannock, York, and James River Estuaries, while depth coverage is good for the Susquehanna, Patuxent, Potomac, and Chester River Estuaries (Table S1). Seasonal coverage (not shown) is excellent for most tidal tributaries. Long-term coverage is excellent for the Potomac River Estuary, with 24 stations having records of about 30 years in length, and the single Chester River Estuary station has a 20-year record. The remaining subestuaries each have at least one station with between 5 and 9 years of continuous measurements.

For certain analyses, a subset of the whole processed data set was created so that robust mean annual cycles and multiyear averages could be computed over a common time period in each tidal tributary. This “reduced data set” was created mainly by selecting stations with good seasonal coverage in the main channels of the tidal tributaries, by limiting the data to the upper 5 m, and by an additional outlier-removal step. The data were then averaged by month, gap filled, and averaged over multiple years to create mean annual cycles. Locations of the stations in the reduced data set are shown in Figure 1a. Further details are provided in supporting information Text S1 and Table S3.

Alkalinity is defined as the excess charge of proton acceptors over proton donors for a reference pK of 4.5 (Dickson, 1981). As such, the common expression for the alkalinity of seawater includes a series of ions, such as bicarbonate, carbonate, and borate. However, while alkalinity is conservative with respect to temperature, salinity, and pressure, the individual ions that make it up are not. Furthermore, the alkalinity of a mixture of two water samples with different alkalinity will obey a linear mixing rule while the individual ions will not (Wolf-Gladrow et al., 2007). Hence, the composition of alkalinity in its traditional definition is not very useful when trying to determine the processes that affect the alkalinity. In this regard, the more useful definition, which is derived from the charge balance, is the explicit conservative alkalinity (Wolf-Gladrow et al., 2007):

$$A = [\text{Na}^+] + 2[\text{Mg}^{2+}] + 2[\text{Ca}^{2+}] + [\text{K}^+] + 2[\text{Sr}^{2+}] + \dots - [\text{Cl}^-] - [\text{Br}^-] - [\text{NO}_3^-] - \dots - \text{TPO}_4 + \text{TNH}_3 - 2\text{TSO}_4 - \text{THF} - \text{THNO}_2 \quad (1)$$

where the brackets indicate concentration and the last five terms represent the total forms of phosphate, ammonia (which is mostly ammonium,  $\text{NH}_4^+$ ), sulfate, fluoride, and nitrite (which is mostly nitrite,  $\text{NO}_2^-$ ), respectively. Among the ions in equation (1), those involving calcium, nitrogen, and sulfur are the most likely to be responsible for nonconservative alkalinity behavior in estuaries. The Chesapeake Bay Program’s regular measurements of the relevant nitrogen ions allowed us to isolate the impact of nitrogen cycling on changes in alkalinity. We thus define the *nitrogenous explicit conservative alkalinity* as  $A_N = [\text{NH}_4^+] - [\text{NO}_3^-] - [\text{NO}_2^-]$ . Then the *nonnitrogenous explicit conservative alkalinity* is defined as  $A - A_N$ , similar to the potential alkalinity of Brewer et al. (1975), changes of which are likely to result from changes in the calcium ion and total sulfate. In what follows, we leave off the qualifier “explicit conservative.” Details of the nitrogen data used to compute  $A_N$  are provided in supporting Text S1 and Tables S1 and S3.

## 2.2. Water Chemistry Data in the Nontidal Rivers

Riverine alkalinity and streamflow data were derived from seven gauging stations of the United States Geological Survey (Figure 1a and Table S4). The Weighted Regressions on Time, Discharge, and Season model (Hirsch et al., 2010) was used to estimate daily concentrations and fluxes of alkalinity, from which the effective monthly mean and long-term mean alkalinity was determined by dividing the flux by the streamflow. Some minor extrapolation of the riverine alkalinity for four of the tidal tributaries was conducted by using the relationship between alkalinity and streamflow. To quantify the influence of nitrogen cycling on riverine alkalinity, Weighted Regressions on Time, Discharge, and Season estimates of monthly mean nitrate + nitrite concentration and ammonium measurements from the Chesapeake Bay Program were used. Full details of the processing of the riverine water chemistry data are provided in supporting information Text S2.



**Table 1**  
*Characteristics of Alkalinity of Rivers Entering the Chesapeake Bay During 1985–1999*

River	Actual long-term mean <sup>a</sup> (mmol m <sup>-3</sup> )	Effective long-term mean <sup>b</sup> (mmol m <sup>-3</sup> )	Coefficient of variation	Variance fraction due to annual cycle	Variance fraction due to streamflow <sup>c</sup>
Susquehanna	900	771	0.19	0.57	0.94
Patuxent	862	751	0.20	0.33	0.90
Potomac	1573	1304	0.19	0.49	0.83
Rappahannock	390	322	0.23	0.30	0.82
Mattaponi	176	135	0.34	0.47	0.87
Pamunkey	387	283	0.35	0.45	0.97
James	1033	859	0.23	0.43	0.91

<sup>a</sup>Average of effective monthly mean concentrations. <sup>b</sup>Long-term (1985–1999) mean flux divided by long-term mean streamflow. <sup>c</sup>Using a power law fit.

### 2.3. Estimation of Alkalinity Sources and Sinks in Tidal Tributaries

Two standard techniques were applied to estimate sources and sinks of alkalinity in the tidal tributaries: the apparent zero-salinity endmember (AZE, Regnier et al., 1998) approach and the mass-balance box model (Officer, 1980). Brief outlines of the applications of these approaches are given here; full details are provided in supporting information Text S3. In the AZE approach, the net biogeochemical source of alkalinity  $\bar{J}$  is determined from riverine discharge, riverine alkalinity, and estuarine alkalinity at various salinities. Due to the steady-state limitations of the method, a single, time-averaged value of  $\bar{J}$  was computed for each tidal tributary. In the box model approach  $\bar{J}$  was computed from 1986 to 2013 at monthly resolution in a single-box configuration of the Potomac River Estuary, where data coverage in space and time is excellent. The box model approach determines the full, time-dependent budget of alkalinity in the box, explicitly estimating the terms for the time rate of change, advection, and turbulent diffusion, and calculating  $\bar{J}$  as a residual. Boundaries for the AZE and box models are shown in Figures 1a and 1b, respectively.

### 2.4. Potomac River Estuary Bivalve and Seagrass Data Analysis

To place the box model results into the context of potential biological processes affecting alkalinity, data on bivalve biomass (ash-free dry mass) and submerged aquatic vegetation (SAV) coverage were analyzed (see supporting information Text S4 for full details). The bivalve biomass data are from the Chesapeake Bay Program and are based on measurements from August to October at fixed and random stations. Two fixed stations, 36 and 40, are located within the boundary of the box model in tidal fresh and oligohaline waters, respectively (Figure 1b). Data from these stations were used to compute the calcification rate following the model of Chauvaud et al. (2003) in which calcification is proportional to ash-free dry mass. The random stations were used to determine how representative the fixed stations are of their respective regions (Boxes 1 and 2 in Figure 1b). Areal coverage of SAV was estimated for Boxes 1 and 2 using data from the Virginia Institute of Marine Science long-term aerial imagery monitoring dataset for the Chesapeake Bay (Orth et al., 2018). Finally, correlations were computed between box model estimates of calcification and the biological metrics (bivalve biomass and SAV coverage).

## 3. Results

### 3.1. Variability of Alkalinity of the Nontidal Rivers

The most striking feature of the alkalinity of the seven main rivers entering the Chesapeake Bay is the nearly order-of-magnitude variation of the long-term mean alkalinity among the rivers, with the lowest mean alkalinity in the Mattaponi River and highest in the Potomac River (Table 1 and Figure 2). This is true regardless of whether the long-term mean is computed by averaging the effective monthly means or by dividing the long-term mean flux by the long-term mean streamflow (the effective long-term mean). Elevation appears to be a driver of the alkalinity variation across the seven gauges. Both types of alkalinity means have the same degree of positive correlation with the mean elevation of the watershed that drains to a given gauge ( $r = 0.7$ ,  $n = 7$ ), presumably reflecting hydrogeomorphic variations within the Chesapeake Bay watershed, with coastal-plain lithology at low elevations and carbonate and siliciclastic lithology at high elevations.

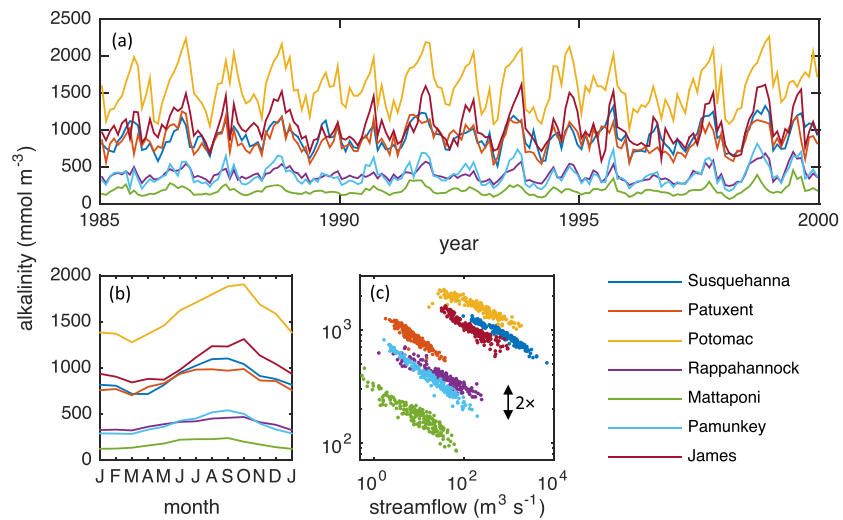


**Figure 2.** Alkalinity at gauges of rivers entering the tidal tributaries of the Chesapeake Bay, 1985–1999. (a) Monthly mean (tick marks represent January 1). (b) Mean annual cycle. (c) Scatterplot of monthly alkalinity vs. monthly streamflow. Arrow shows factor of 2 range. Locations of river gauges are given in Figure 1a and Table S4.

Temporal variability is substantial (Figure 2a), with the coefficient of variation (standard deviation divided by the mean) varying between 0.19 and 0.35 (Table 1). The full range of monthly mean alkalinity within a river is typically a factor of 2 but can be as high as a factor of 4 (e.g., for the Mattaponi River; Figure 2c). Much of the temporal variability is due the mean annual cycle (Figure 2b), which accounts for 30% to 57% of the variability of monthly mean alkalinity (Table 1). A major control on the annual cycle of alkalinity is the negative relationship between streamflow and alkalinity (Figure 2c), which accounts for 82% to 97% of variability of the full monthly time series from 1985 to 1999 (Table 1). Weathering products, such as alkalinity, typically have greatest concentration when streamflow is low (Godsey et al., 2009). This pattern is a result of the contribution of long-residence-time groundwater to base flow in streams. The increased contact time allows weathering products to accumulate, resulting in high concentrations when streamflow is low. When streamflow is high, these weathering products are diluted by short-residence-time water, such as stormflow and overland runoff. Surface runoff in temperate climates is highest in the spring and lowest in the fall. Thus, the alkalinity annual cycle is characterized by a minimum in March for most rivers (April for the Susquehanna River and January for the Mattaponi River) and a maximum in September or October. For a given river, the minimum alkalinity occurs during the month of maximum discharge, except for the Mattaponi River, when the minimum occurs 2 months earlier. Similarly, the alkalinity maximum in the mean annual cycle occurs close to the month of minimum discharge, lagging it by 1 or 2 months. The anticorrelation between flow and alkalinity makes the effective long-term-mean alkalinity lower than the actual long-term mean alkalinity by 14% to 27% (Table 1).

Nitrogen cycling was found to have a small impact on river alkalinity. The range in the 1985–1999 mean alkalinity among the rivers is 1397 mmol m<sup>-3</sup> (Potomac minus Mattaponi), while the corresponding range in nitrate + nitrite is only 133 mmol m<sup>-3</sup>. Similarly, the temporal variability in alkalinity, as given by the standard deviation of monthly mean values, is more than an order of magnitude greater than the temporal variability in nitrate + nitrite, except for the Patuxent (factor of 4 higher) and Rappahannock (factor of 7 higher) Rivers. Because a monthly mean ammonium product was not available for the River Input Monitoring stations (supporting information Text S2), we assessed the contribution from ammonium by computing the mean and standard deviation of all the ammonium measurements from the Chesapeake Bay Program from 2012 to 2017 (the period when sufficient data were available) at each river gauging station (Table S4). These were compared to corresponding means and standard deviations of the River Input Monitoring nitrate + nitrite data over the same time period. The ratio (ammonium divided by the sum of nitrate + nitrite) of the means varied from 0.02 to 0.14 and the ratio of the standard deviations from 0.08 to 0.52. Hence, the impact of ammonium on alkalinity is even smaller than that of nitrate + nitrite.



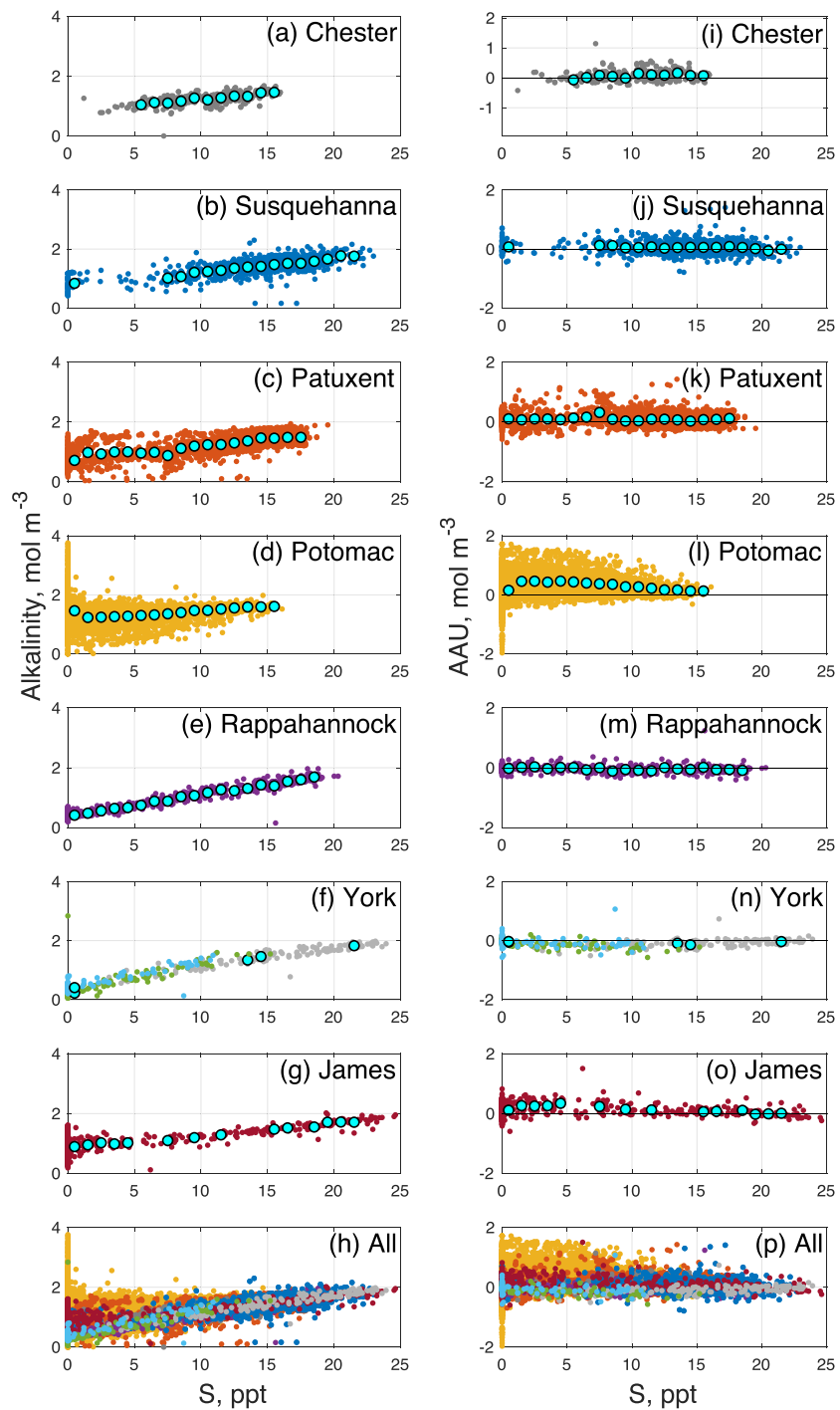


**Figure 3.** (a–h) Alkalinity and (i–p) apparent alkalinity utilization (AAU) versus salinity for each and all of the tidal tributaries for the whole processed data set (Table S2). In the York panels, the Pamunkey River Estuary is in blue, the Mattaponi River Estuary is in green, and downstream of the confluence is in gray. For the individual tidal tributaries, averages in salinity bins of 1 are shown as circles when 10 or more data points are in the bin.

### 3.2. Variation of Alkalinity With Salinity in the Tidal Tributaries

The left panels of Figure 3 (a–h) show how alkalinity varies with salinity in each tidal tributary. As is often found in estuaries, alkalinity generally increases with salinity as a result of mixing between a freshwater end-member of relatively low alkalinity and an oceanic end-member of relatively high alkalinity. Atlantic Ocean

**Table 2**  
*Statistics for Alkalinity in the Tidal Tributaries*

Tidal tributary	Mean tidal-fresh alkalinity ( $\text{mmol m}^{-3}$ ) <sup>c</sup>	Instantaneous mixing model	
		RMS <sup>d</sup> error ( $\text{mmol m}^{-3}$ )	Coefficient of determination, $r^2$
Susquehanna	838	207	0.43
Patuxent	714	225	0.56
Potomac	1461	435	-0.42
Rappahannock	413	111	0.93
York <sup>a</sup>	--	159	0.83
Mattaponi <sup>b</sup>	222	244	0.65
Pamunkey <sup>b</sup>	408	183	0.66
James	895	238	0.55

Note. For the instantaneous mixing model, a high-salinity endmember of  $S_{HS} = 20$  and  $A_{HS} = 1,700 \text{ mmol m}^{-3}$  was used.

<sup>a</sup>Downstream of the confluence of the Mattaponi and Pamunkey River Estuaries. <sup>b</sup>Upstream of the confluence of the Mattaponi and Pamunkey River Estuaries. <sup>c</sup>Computed as the mean of all data of salinity <1. <sup>d</sup>Root-mean-square.

water at the mouth of Chesapeake Bay, where the salinity is approximately 32, has an alkalinity of approximately  $2,200 \text{ mmol m}^{-3}$  (Wong, 1979), which is greater than the mean alkalinity of each river entering the Bay (Table 1). The main exception to this generality is the Potomac River Estuary, where the highest alkalinity is found at the lowest salinity. Tidal fresh (salinity < 0.5), oligohaline ( $0.5 < \text{salinity} < 5$ ), and mesohaline ( $5 < \text{salinity} < 18$ ) conditions are captured to some extent in all of the tidal tributaries. Polyhaline conditions ( $18 < \text{salinity} < 30$ ) are found in the York and James River Estuaries (Figures 3f and 3g), owing to their proximity to the ocean, and the Susquehanna River Estuary (Figure 3b), owing to the sampling of waters as deep as 18 m at the southernmost station in that system.

The alkalinity data were averaged in salinity bins of 0–1, 1–2, etc., when there were 10 or more measurements in a bin. This binning reveals that with declining salinity, the mean alkalinity approaches the mean riverine endmember. For example, the Mattaponi and Potomac River Estuaries (Figures 3f and 3d) have mean alkalinities (where the averages were computed for all available data) in the 0–1 salinity bin of 222 and  $1,461 \text{ mmol m}^{-3}$  (Table 2), respectively, which roughly mimic the mean 1985–1999 values of the corresponding rivers: 176 and  $1,573 \text{ mmol m}^{-3}$  (Table 1). There are not enough low-salinity data for the single station in the Chester River Estuary, but a linear fit to the data (the majority of which are between salinities of 5 and 15) in Figure 3a gives a zero-salinity intercept of  $789 \text{ mmol m}^{-3}$ . We suggest that exchange with the Susquehanna River Estuary has a large impact on the alkalinity at this station because the station is only about 10 km from the mouth of the Chester River Estuary and the mean streamflow of the Chester River, about  $20 \text{ m}^3 \text{ s}^{-1}$  (Tian, 2019), is more than 2 orders of magnitude smaller than that of the Susquehanna River. Indeed, the zero-salinity intercept is only 3% higher than the 1985–1999 effective long-term mean alkalinity of the Susquehanna River (Table 1), which supports our suggestion.

All of the tidal tributaries converge to a common value of alkalinity at high salinity (Figure 3h). The convergence can be quantified by considering the binned alkalinity data. In the 14–15 and 15–16 salinity bins, the mean alkalinity varies among the tidal tributaries from  $1394 \text{ mmol m}^{-3}$  to  $1607 \text{ mmol m}^{-3}$ , or  $\pm 7\%$ . In the three tidal tributaries with a 22–23 salinity bin, the range in these averages is  $1710\text{--}1829 \text{ mmol m}^{-3}$ , or  $\pm 3\%$ . This convergence at high salinity can be contrasted with the large range in the 0–1 salinity bin,  $222\text{--}1,461 \text{ mmol m}^{-3}$  ( $\pm 74\%$ ), and the river gauges (1985–1999 means),  $191\text{--}1,655 \text{ mmol m}^{-3}$  ( $\pm 80\%$ ).

The tidal tributaries differ in the degree to which salinity captures variability in alkalinity (Figures 3a–3h). Although alkalinity in the Chester, Rappahannock, York, and James River Estuaries varies nearly linearly with salinity, the scatter is considerable for the Potomac and Patuxent River Estuaries; the Susquehanna River Estuary lies in between these two extremes. The alkalinity data are not expected to fall along a single line for four reasons. First, the endmembers change with time, particularly the freshwater endmember, as discussed above; this may account for the relatively high scatter at low salinities in some of the tidal tributaries, particularly the Potomac and James River Estuaries (Figures 3d and 3g). Second, there may be biogeochemical sources or sinks of alkalinity in the estuary (e.g., calcification), as suggested by prior research in

these estuaries (see section 1). Third, there may be other freshwater sources (atmospheric precipitation and additional tributaries) to the estuary with levels of alkalinity that differ from the main freshwater source, which is plausible given that the fraction of the watershed that is gauged varies from 0.40 for the Patuxent River Estuary to 0.87 for the Potomac River Estuary (Table S4). Fourth, at any given time, the alkalinity–salinity relationship will depart from linearity if the freshwater endmember is variable and if the time scale for river water to reach a certain location within an estuary (transport time scale) is comparable to or longer than the time scale of variability in the freshwater endmember (Cifuentes et al., 1990; Loder & Reichard, 1981). A rough estimate of the transport time scale is the estuarine volume divided by the mean freshwater input, which varies between 1 month for the Potomac and Rappahannock River Estuaries to 9 months for the Patuxent River Estuary (Table S4).

If the transport time scale is relatively short and there are no biogeochemical or other alkalinity sources and sinks, then the alkalinity in an estuary is simply a result of the instantaneous mixing of the fresh and high-salinity endmembers. To assist in the analysis of the alkalinity data, we computed the alkalinity due to instantaneous mixing as

$$A_{IM} = \left(1 - \frac{S}{S_{HS}}\right)A_R + \frac{S}{S_{HS}}A_{HS} \quad (2)$$

where  $S$  is the observed salinity,  $A_R$  is the alkalinity of the riverine endmember corresponding to the time of observation (section 2.2), and  $S_{HS}$  and  $A_{HS}$  are the salinity and alkalinity, respectively, of a fixed high-salinity endmember (the same for all estuaries). For the York River Estuary downstream of the confluence of its two major tributaries (Mattaponi and Pamunkey), the value of  $A_R$  was computed as a flow-weighted mean of the two rivers. We considered three different values of  $S_{HS}$  (15, 20, and 25) and used alkalinity–salinity relationships (Figure 3) to select corresponding values of  $A_{HS}$  equal to 1,450, 1,700, and 2,000 mmol m<sup>−3</sup>.

The degree to which  $A_{IM}$  can describe the alkalinity data (Figures 3a–3h) varies dramatically among the tidal tributaries (Table 2). Results are presented for  $S_{HS} = 20$ ; similar results were found for  $S_{HS} = 15$  and 25. The tidal tributary that is best explained by instantaneous conservative mixing is the Rappahannock River Estuary, where 93% of the variability can be accounted for (Table 2). This tributary has a short mean residence time (1 month; Table S4) and it is therefore not surprising that its alkalinity distribution is well explained by instantaneous conservative mixing. On the other hand, in the other tributary with a short residence time, the Potomac River Estuary, alkalinity is poorly explained by instantaneous conservative mixing; the coefficient of determination is actually negative, indicating that the mean of  $A$  is a better representation of the data than is  $A_{IM}$ . Hence, nonconservative behavior may be important in this system. The York River Estuary and its tidal tributaries also are well explained by  $A_{IM}$ , with 65 to 83% of the variability accounted for. The Susquehanna, Patuxent, and James River Estuaries have a moderate amount (43% to 56%) of their alkalinity variability explained by instantaneous mixing. The apparent alkalinity utilization,  $AAU = A_{IM} - A$ , reveals the deviations between the alkalinity and expectations from instantaneous mixing (Figures 3i–3p). The Potomac and James River Estuaries show a clear tendency for positive values of  $AAU$ , suggesting an alkalinity sink. Focusing on individual data points for the York River Estuary (there are not enough data to compute more than four averages in salinity bins), it is clear that  $AAU$  is generally negative, suggesting an alkalinity source. The remaining tidal tributaries do not show a clear pattern of  $AAU$ .

Evidence for nonconservative behavior in alkalinity is more clearly suggested when the salinity and alkalinity data are averaged over time for each station and then plotted against each other (Figure 4a). The concave-upward structure, particularly in the Potomac, James, and Patuxent River Estuaries, is suggestive of an alkalinity sink. A similar pattern is apparent to a lesser extent for the Rappahannock and possibly Susquehanna River Estuaries, whereas the Mattaponi and Pamunkey River Estuaries have a slight concave-downward structure, suggesting an alkalinity source.

Contributions of nitrogenous alkalinity ( $A_N$ ) to the total alkalinity are small, as can be seen from a comparison of Figure 4b with Figure 4a (note the different vertical scales). At a salinity of 5, for example,  $A_N$  is, on average, less than 5% of the total alkalinity. As with total alkalinity,  $A_N$  increases with salinity, reflecting mixing between a low- $A_N$  fresh water endmember and a high- $A_N$  high-salinity endmember. The linearity of the  $A_N$ -vs- $S$  plots for the Potomac, Susquehanna, Mattaponi, and James River Estuaries suggests

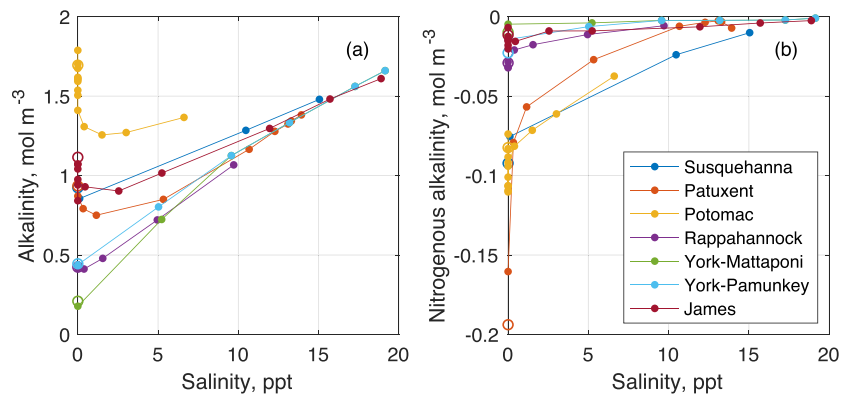


**Figure 4.** Temporal averages of (a) alkalinity and (b) nitrogenous alkalinity vs. temporal averages of salinity for each of the tidal tributaries using the reduced data set (Table S3). Each data point represents a station. The open circles are the averages at the river gauges (Table S4). Note the different vertical scales.

conservative behavior for  $A_N$  in these systems. On the other hand, the concave-downward structure for the Patuxent, Rappahannock, and Pamunkey River Estuaries suggests a source of  $A_N$  in these systems, reflecting some combination of a nitrate sink, a nitrite sink, and an ammonium source. The Patuxent River Estuary stands out as having a particularly large apparent  $A_N$  source. In this system, for example, total alkalinity decreases, on average, by  $0.18 \text{ mmol m}^{-3}$  from the river gauge to the station with a mean salinity of 1.2, whereas  $A_N$  increases between these two locations by  $0.13 \text{ mmol m}^{-3}$ . Hence, the alkalinity sink in the Patuxent River Estuary due to processes not involving nitrogen (e.g., calcification) may be  $0.13 + 0.18 = 0.31 \text{ mmol m}^{-3}$ , about 70% larger than what is suggested by the total alkalinity distribution alone. Summarizing, while  $A_N$  may be relatively low compared to total alkalinity, gradients in  $A_N$  can be large, at least in some tidal tributaries, indicating that processes involving nitrogen can play a role in the alkalinity distribution.

### 3.3. Mean Annual Cycle of Alkalinity in the Tidal Tributaries

The mean annual cycles of alkalinity in the seven tidal tributaries (based on the reduced data set; Table S3) show some similar behavior in their most upstream portions, within approximately 40 km of the river gauge; the imprint of the river is clear in that the annual cycles have minima in late winter and early spring and maxima in late summer and early fall (Figures 5a–5g). This phasing of the annual cycle is also evident in the most downstream portions of most of the tidal tributaries, where the annual cycles look very similar to those of salinity (not shown). Hence, both the seasonality in the low-alkalinity water from rivers and the seasonality of the intrusion of high-alkalinity water of marine origin can work constructively to increase the amplitude of the mean annual cycle. The only exception is the Potomac River Estuary (Figure 5c), where the annual cycle in the most downstream station has a weak maximum in late fall and weak minimum in late spring.

It is in the central portions of the tidal tributaries where the mean annual cycles differ the most among the tidal tributaries. The Rappahannock, Mattaponi, and Pamunkey River Estuaries fall into one group that is characterized by nearly monotonically increasing alkalinity in the downstream direction and mean annual cycles with phasing similar to the upstream and downstream portions of the tidal tributaries (Figures 5d–5f). In the other four tidal tributaries, alkalinity minima are present. The Potomac River Estuary minimum is the most noticeable and is centered about 80 km downstream of the gauge during summer (Figure 5c). Minima are centered in the late winter or early spring in the Susquehanna, Patuxent, and James Rivers, roughly 30, 40, and 130 km, respectively, downstream of the gauge (Figures 5a, 5b, and 5g). Minima are present in these three tidal tributaries in other seasons as well.

The apparent alkalinity utilization makes further distinctions among the tidal tributaries (Figure 5h–5n) that go beyond the AAU plots that do not consider seasonality (Figures 3i–3p). At one extreme is the Potomac River Estuary, which has a very large AAU maximum (exceeding  $700 \text{ mmol m}^{-3}$ ; Figure 5j) centered at the same location as the alkalinity minimum (Figure 5c), strongly suggestive of a summertime

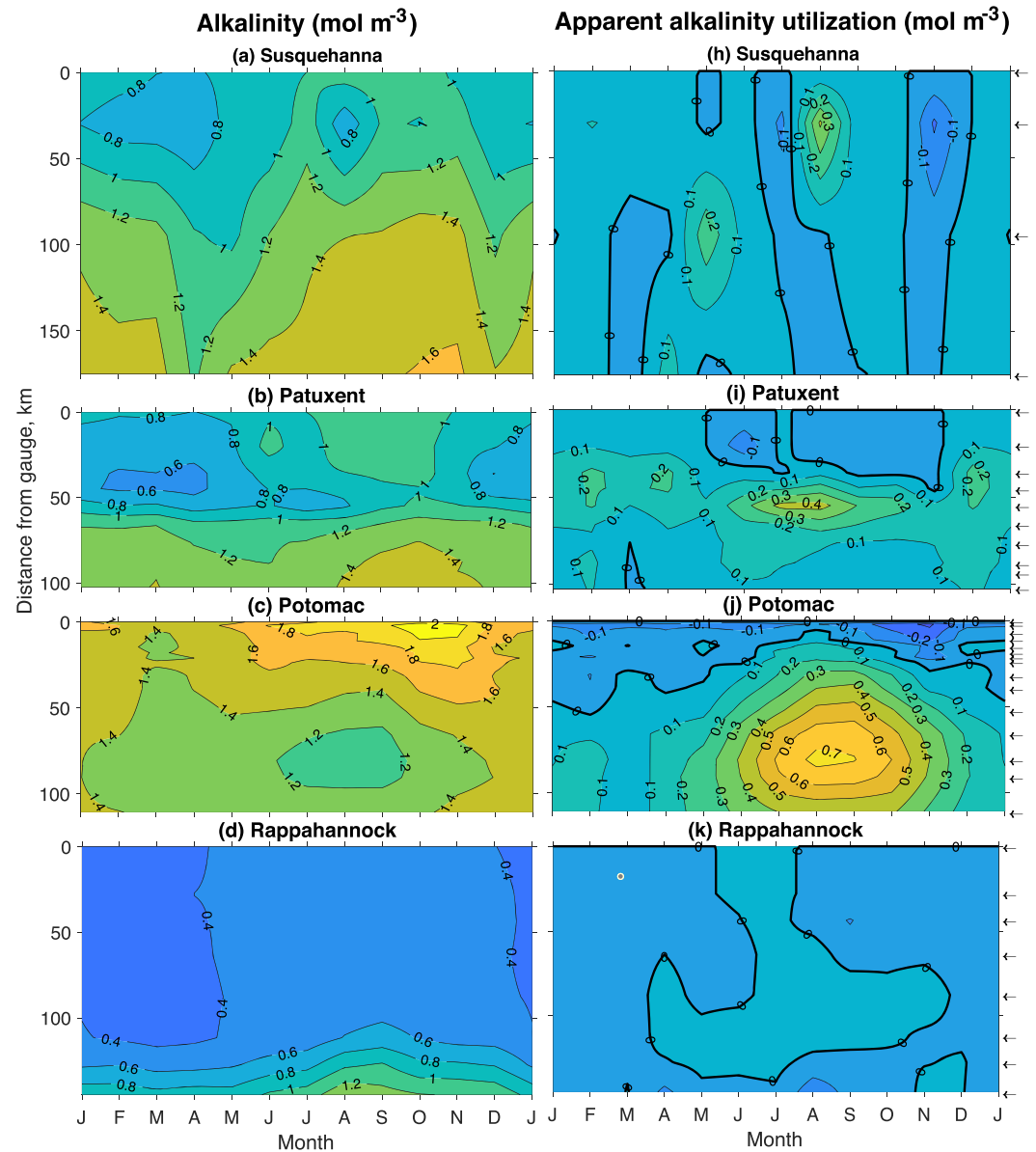


**Figure 5.** Mean annual cycles of (a–g) alkalinity and (h–n) apparent alkalinity utilization in the seven tidal tributaries as a function of distance from the river gauge (Table S4). This analysis is based on the reduced data set (Table S3). Station locations are indicated by arrows at the far right.

alkalinity sink throughout much of the tidal tributary. At the other extreme is Rappahannock River Estuary, where AAU is extremely low everywhere, indicating the likelihood of conservative mixing in this system (Figure 5k), consistent with Figure 3m. The Susquehanna River Estuary is most like the Rappahannock River Estuary, with relatively low (but noisy) AAU (Figure 5h). The other tidal tributaries show indications of modest sources or sinks, or perhaps a significant time for the river signal to be felt in the estuary due to longer residence times (Table S4). For example, the Mattaponi and Pamunkey River Estuaries have distinct negative AAU minima centered around 60 and 130 km, respectively (Figures 5l and 5m), suggesting alkalinity sources. AAU is mostly positive in the Patuxent River Estuary (Figure 5i) and is similar in character to the Potomac River Estuary, with the sink centered in summer and some indication of a source (negative AAU) upstream within 20–40 km of the gauge. The James River Estuary also has a combination of implied sources and sinks, but the separation is temporal, with negative AAU

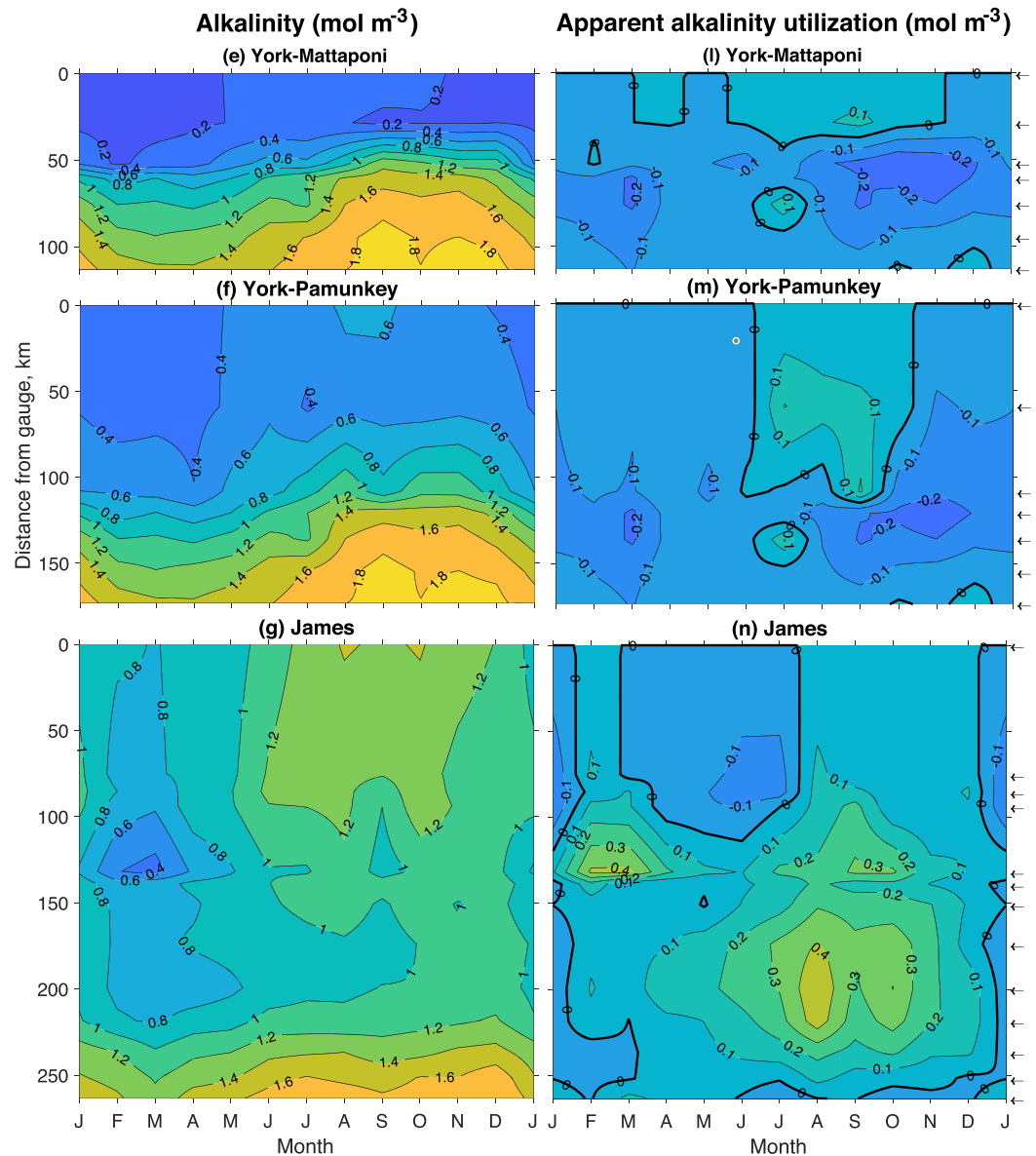


Figure 5. (continued)

(suggestive of a source) in late spring and early summer and positive AAU (suggestive of a source) for the rest of the year.

### 3.4. Long-Term Trends in Alkalinity in the Tidal Tributaries

At all 25 stations where alkalinity has been measured for two decades or more, long-term increasing trends are present with  $p < 0.05$  (Table 3). To make the trends comparable among the stations, the trend analysis was limited to data shallower than 5 m and to 2012 and earlier. Fourteen of the stations are along the main axis of the Potomac River Estuary, 10 are in small tributaries that drain to the Potomac River Estuary (seven in the Anacostia River and one each in Washington Channel, Piscataway Creek, and Mattawoman Creek), and 1 is in the Chester River Estuary (which drains to the Susquehanna River Estuary). Figure 6 shows time series from selected stations.

The 24 Potomac-related stations (see Figure 1b for station locations) have large trends, varying from 5.6 to 20.8 mmol m<sup>-3</sup> year<sup>-1</sup>, which are all greater than the trend of the Potomac River itself (~5 mmol m<sup>-3</sup> year<sup>-1</sup>, Table 3). The 14 mainstem Potomac stations have a median trend of 12.6 mmol m<sup>-3</sup> year<sup>-1</sup> and 10



**Table 3**  
*Linear Alkalinity Trend Statistics for Long-Term Stations*

Station	Period	Trend <sup>h</sup> (mmol m <sup>-3</sup> year <sup>-1</sup> )	<i>p</i> value	Nitrogen fraction of trend
Potomac River	1984–2012	5.4 ± 1.6	<0.001	0.16
Potomac River	1986–2009	4.7 ± 2.1	0.023	0.20
PMS01 <sup>a</sup>	1984–2012 <sup>g</sup>	20.8 ± 3.2	<0.001	0.02
PMS10 <sup>a</sup>	1984–2012 <sup>g</sup>	12.8 ± 2.4	<0.001	0.03
PMS21 <sup>a</sup>	1984–2012 <sup>g</sup>	13.0 ± 2.3	<0.001	0.01
PMS29 <sup>a</sup>	1984–2012 <sup>g</sup>	13.0 ± 2.2	<0.001	0.04
PMS37 <sup>a</sup>	1984–2012 <sup>g</sup>	13.4 ± 2.8	<0.001	0.15
PMS44 <sup>a</sup>	1984–2012 <sup>g</sup>	13.7 ± 2.8	<0.001	0.07
PMS51 <sup>a</sup>	1984–2012 <sup>g</sup>	15.6 ± 2.7	<0.001	0.11
TF2.1 <sup>a</sup>	1986–2009	10.9 ± 1.9	<0.001	0.31
TF2.2 <sup>a</sup>	1986–2009	11.9 ± 1.4	<0.001	0.26
TF2.3 <sup>a</sup>	1986–2009	12.5 ± 1.3	<0.001	0.19
TF2.4 <sup>a</sup>	1986–2009	11.6 ± 1.4	<0.001	0.18
RET2.1 <sup>a</sup>	1986–2009	11.2 ± 1.8	<0.001	0.16
RET2.2 <sup>a</sup>	1986–2009	11.8 ± 1.1	<0.001	0.13
RET2.4 <sup>a</sup>	1986–2009	11.7 ± 1.0	<0.001	0.10
ANA01 <sup>b</sup>	1984–2012 <sup>g</sup>	10.5 ± 1.7	<0.001	0.06
ANA05 <sup>b</sup>	1984–2012 <sup>g</sup>	7.1 ± 2.2	0.001	NA
ANA08 <sup>b</sup>	1984–2012 <sup>g</sup>	6.0 ± 2.2	0.006	0.04
ANA11 <sup>b</sup>	1984–2012 <sup>g</sup>	5.8 ± 2.3	0.012	NA
ANA14 <sup>b</sup>	1984–2012 <sup>g</sup>	5.6 ± 1.7	0.001	–0.11
ANA24 <sup>b</sup>	1984–2012 <sup>g</sup>	9.0 ± 2.8	0.002	NA
ANA29 <sup>b</sup>	1984–2012 <sup>g</sup>	11.6 ± 2.6	<0.001	0.02
PWC04 <sup>c</sup>	1984–2012	9.7 ± 2.7	<0.001	0.01
XFB1986 <sup>d</sup>	1986–2009	10.5 ± 2.2	<0.001	0.30
MAT0016 <sup>e</sup>	1986–2009	7.9 ± 2.1	<0.001	0.12
Susquehanna River	1986–2005	2.7 ± 1.9	0.14	0.35
XGG8251 <sup>f</sup>	1986–2005	4.9 ± 1.9	0.011	–0.03

*Note.* Data deeper than 5 m were not included. The Potomac and Susquehanna River stations are the same as those in Table S4.

<sup>a</sup>Along the main axis of the Potomac River Estuary. <sup>b</sup>In the Anacostia River Estuary. <sup>c</sup>In the Washington Channel. <sup>d</sup>In Piscataway Creek. <sup>e</sup>In Mattawoman Creek. <sup>f</sup>In the Chester River Estuary. <sup>g</sup>2009 is missing. <sup>h</sup>±1 standard error.

of the stations have very similar trends, falling between 11.6 and 13.7 mmol m<sup>-3</sup> year<sup>-1</sup> (e.g., Figures 6a–6c). The trends at the two most downstream stations in the Anacostia River, the Washington Channel station, and the two tidal creek stations are somewhat lower, varying between 7.9 and 11.6 mmol m<sup>-3</sup> year<sup>-1</sup> (e.g., Figure 6d); we suspect that these upward trends are driven mainly by exchange with the Potomac River Estuary because the stations are only a few km from the mouths of these tributaries and the mean stream-flow of each tributary (determined from StreamStats) is more than two orders of magnitude smaller than that of the Potomac River. Trends further upstream in the Anacostia River are somewhat lower, with a median of 6.0 mmol m<sup>-3</sup> year<sup>-1</sup>. Closer examination of the upstream Anacostia River time series reveals fairly constant alkalinity from 1984 to 1997, relatively high alkalinity from 1998 to 2001, and a weak decline or constant values from 2002 to 2012 (Figure 6e).

What could be responsible for the trends in the Potomac River Estuary and its tributaries? The relatively small trend in the river endmember rules out watershed alkalinity changes as the primary driver. Changes in the mixture of river water with high-salinity water are also unlikely, as these would lead to salinity trends, which were found to be insignificant at all of the stations. Changes in nitrogenous alkalinity were found to contribute significantly to the alkalinity trends, accounting for 10 to 30% of the trend, a contribution that decreases monotonically in the downstream direction (Table 3). Examination of individual contributions to the nitrogenous alkalinity trend revealed that a decline in the nitrate concentration is the main cause of the trend; the contributions of nitrate, nitrite, and ammonium to the nitrogenous alkalinity trends are 105% to 112%, 3% to 6%, and –12% to –16%. Declining nitrate levels are, in turn, very likely a result of declining loads from wastewater treatment plants (Bricker et al., 2014; Karrh et al., 2013). This leaves

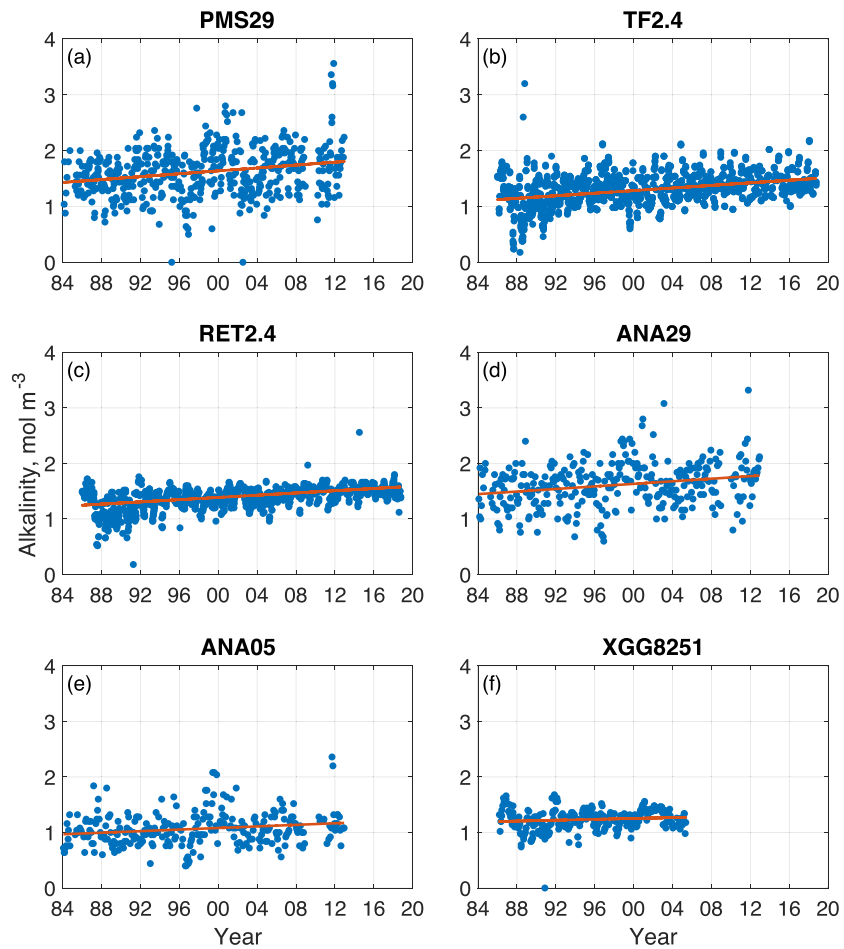


**Figure 6.** Alkalinity as a function of time and linear trends at selected long-term estuarine stations (Table 3): (a–c) Potomac River Estuary, (d–e) Anacostia River Estuary, and (f) Chester River Estuary.

**Table 4**

*Inputs and Outputs of the Apparent Zero-Salinity-Endmember Model for Estimating Total and Nonnitrogenous Alkalinity Sources and Sinks in Chesapeake Bay Tidal Tributaries*

	Tidal tributary	$C_0$ ( $\text{mmol m}^{-3}$ )	$C_R$ ( $\text{mmol m}^{-3}$ )		$\bar{J}V/\alpha$ ( $\text{mmol m}^{-2} \text{d}^{-1}$ )		$\bar{J}V/QC_R$ (%)	
			Act	Eff	Act	Eff	Act	Eff
Total alkalinity	Susquehanna	$730 \pm 51$	924	821	$-21 \pm 6$	$-10 \pm 6$	$-21 \pm 6$	$-11 \pm 6$
	Patuxent	$565 \pm 59$	935	776	$-19 \pm 3$	$-11 \pm 3$	$-40 \pm 6$	$-27 \pm 8$
	Potomac	$1,189 \pm 23$	1695	1404	$-48 \pm 3$	$-20 \pm 2$	$-30 \pm 1$	$-15 \pm 2$
	Rappahannock	$426 \pm 64$	424	317	$0 \pm 3$	$5 \pm 3$	$0 \pm 15$	$34 \pm 20$
	Mattaponi	$372 \pm 71$	209	137	$11 \pm 5$	$15 \pm 5$	$78 \pm 34$	$171 \pm 52$
	Pamunkey	$457 \pm 65$	445	284	$1 \pm 5$	$12 \pm 5$	$3 \pm 15$	$61 \pm 23$
	James	$778 \pm 44$	1,115	846	$-25 \pm 3$	$-5 \pm 3$	$-30 \pm 4$	$-8 \pm 5$
Nonnitrogenous alkalinity	Susquehanna	$801 \pm 47$	1016	917	$-23 \pm 5$	$-13 \pm 5$	$-21 \pm 5$	$-13 \pm 5$
	Patuxent	$592 \pm 57$	1129	939	$-27 \pm 3$	$-17 \pm 3$	$-48 \pm 5$	$-37 \pm 6$
	Potomac	$1273 \pm 16$	1777	1500	$-48 \pm 2$	$-22 \pm 2$	$-28 \pm 1$	$-15 \pm 1$
	Rappahannock	$436 \pm 64$	453	355	$-1 \pm 3$	$4 \pm 3$	$-4 \pm 14$	$23 \pm 18$
	Mattaponi	$346 \pm 73$	219	147	$8 \pm 5$	$13 \pm 5$	$58 \pm 34$	$136 \pm 50$
	Pamunkey	$457 \pm 67$	468	303	$-1 \pm 5$	$11 \pm 5$	$-2 \pm 14$	$51 \pm 22$
	James	$795 \pm 44$	1127	862	$-24 \pm 3$	$-5 \pm 3$	$-29 \pm 4$	$-8 \pm 5$

*Note.* Uncertainties are standard errors.  $C_0$  = alkalinity of apparent zero-salinity endmember;  $C_R$  = effective (Eff) and actual (Act) mean river alkalinity;  $\bar{J}V/\alpha$  = alkalinity source per unit area;  $\bar{J}V/QC_R$  = alkalinity source as a fraction of river input;  $V$  = estuarine volume;  $\alpha$  = estuarine surface area;  $Q$  = streamflow.

between 70% and 90% of the alkalinity trend unaccounted for. Remaining possibilities are increases in the alkalinity of rivers not accounted for by the river endmember, changes in point sources (e.g., wastewater discharge), and changes in internal (e.g., biogeochemical) sources and sinks.

The alkalinity trend of the station in the Chester River Estuary (Figure 6f) is  $4.9 \text{ mmol m}^{-3} \text{ year}^{-1}$ . As argued above (section 3.2), exchange with the Susquehanna River Estuary likely has a large influence on the alkalinity at this station. The mean salinity at the station is 10 and thus may be a mixture of two parts river water and one part ocean water of salinity 30. Assuming conservative mixing and a stationary ocean endmember, the alkalinity trend of the Susquehanna River would need to be  $7.4 \text{ mmol m}^{-3} \text{ year}^{-1}$  in order to account for the observed trend at the station. However, the actual trend at the Susquehanna River is less than half of this value and is not significant (Table 3). An increasing contribution of a high-salinity, high-alkalinity endmember is also ruled out because the station salinity has no trend. Finally, the contribution of nitrogenous alkalinity at the station is insignificant. It thus appears that, similar to the Potomac River Estuary trends, a change in some nonconservative process (or lateral inputs not accounted for) are needed to account for the alkalinity trend of the Chester River Estuary station. Nonconservative processes are explored in more detail in the next section.

### 3.5. Sources and Sinks of Alkalinity in the Tidal Tributaries

#### 3.5.1. Apparent Zero-End-Member Approach

Application of the apparent zero-salinity endmember approach (section 2.3 and supporting information Text S3) using the effective long-term mean river alkalinity yielded estimates of an alkalinity sink in the Susquehanna, Patuxent, Potomac, and James River Estuaries, and an alkalinity source in the Mattaponi, Pamunkey, and Rappahannock River Estuaries (Table 4). On a unit area basis, the Potomac River Estuary is the largest sink, at  $20 \pm 2 \text{ mmol m}^{-2} \text{ day}^{-1}$ , ( $\pm 1$  standard error) and the Mattaponi River Estuary is the largest source, at  $15 \pm 5 \text{ mmol m}^{-2} \text{ day}^{-1}$ . As a fraction of the river flux, the Patuxent River Estuary is the largest sink, at  $27 \pm 8\%$ , and the Mattaponi River Estuary is the largest source, at  $171 \pm 52\%$ .

Removing the influence of nitrogen reduces the net source, increases the net sink, or has no effect (Table 4), which is consistent with the tidal tributaries acting as net sinks for nitrate (e.g., via algal nitrate uptake and denitrification). This influence, however, is modest, except for the Patuxent River Estuary, where nitrogen is responsible for about one third of the alkalinity sink. These findings are consistent with the relationship between nitrogenous alkalinity and salinity (Figure 4b), which suggests mainly conservative behavior except in the Patuxent River Estuary.

Estimates of nonconservative behavior are very different when the actual mean river alkalinity is used instead of the effective mean river alkalinity (Table 4). For example, the Potomac River Estuary sink is reduced by more than half. However, regardless of the method, the differences among the tidal tributaries in terms of the fraction of river alkalinity consumed are unchanged. In both cases, this fraction increases as the mean river alkalinity increases (Figure 7).

#### 3.5.2. Potomac River Estuary Box Model

The box model calculation for the Potomac River Estuary reveals an alkalinity sink for most (79%) months of the 1986–2013 time series (Figure 8a). The net biogeochemical source, which has a long-term average ( $\pm 1$  standard deviation) of  $-22.0 \pm 24.7 \text{ mmol m}^{-2} \text{ day}^{-1}$ , is highly variable, with monthly estimates ranging from  $-178$  to  $+65 \text{ mmol m}^{-2} \text{ day}^{-1}$ . A linear fit to the monthly estimates reveals a trend ( $\pm 1$  standard error) of  $0.33 \pm 0.17 \text{ mmol m}^{-2} \text{ day}^{-1} \text{ year}^{-1}$  ( $p = 0.05$ ), which equates to a sink reduction of 65% from 1986 to 2013. Annual estimates of the alkalinity budget (Figure 8b) show that the net biogeochemical sink is mainly balanced by an advective source, though in some years mixing is important. The mean annual cycle of the budget (Figure 8c) reveals the period of greatest sink (April–July) occurring when advection is also relatively high and the month of weakest sink (March) occurring when advection is closest to zero. In the mean annual cycle, mixing is a fairly constant source of alkalinity, while the rate of change is of comparable magnitude, revealing substantial decreases in winter and summer and increases in the fall. Averaged over the whole time series, 76% and 24% of the biogeochemical sink is balanced by advection and mixing, respectively.

The net biogeochemical sink ( $-J$ ) is positively correlated to the advective source for the full time series ( $r = 0.79$ ,  $p < 10^{-3}$ ,  $n = 336$ ), annual averages ( $r = 0.88$ ,  $p < 10^{-3}$ ,  $n = 28$ ), and the mean annual cycle ( $r = 0.61$ ,  $p = 0.04$ ,  $n = 12$ ). Is advection driving the biogeochemistry or vice versa? Advection is equal to  $Q(C_R - C_D)$

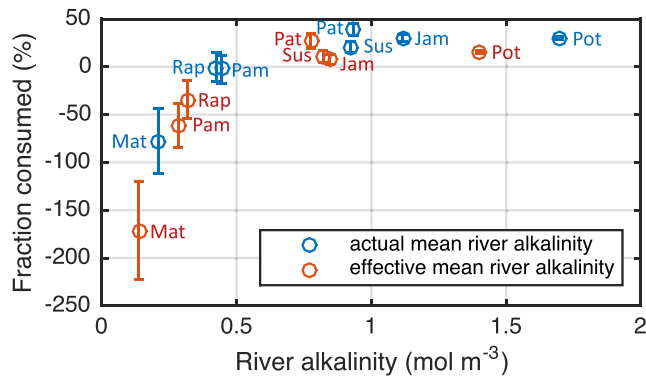


**Figure 7.** The fraction of the riverine total alkalinity input that is consumed in the tidal tributary as a function of riverine alkalinity. Mat = Mattaponi; Pam = Pamunkey; Rap = Rappahannock; Pat = Patuxent; Jam = James; Sus = Susquehanna; Pot = Potomac. Two versions of the calculation are presented, one using the actual mean river alkalinity and the other the effective mean river alkalinity (Table 4).

(supporting information Text S3) and so higher streamflow, higher river alkalinity, and lower downstream alkalinity would favor higher advection. If upstream conditions ( $Q$  and  $C_R$ ) are positively correlated to  $-J$ , then it is reasonable to conclude that advection is driving the biogeochemistry. On the other hand, if downstream conditions ( $C_D$ ) are negatively correlated to  $-J$ , it is more likely that the biogeochemistry is driving the advection. For the full time series,  $-J$  is weakly correlated with  $Q$  ( $r = 0.21$ ,  $p < 10^{-3}$ ), weakly anticorrelated with  $C_R$  ( $r = -0.17$ ,  $p = 0.002$ ), and somewhat more strongly anticorrelated with  $C_D$  ( $r = -0.48$ ,  $p < 10^{-3}$ ). Thus, it appears that the biogeochemistry is driving the advection by influencing downstream conditions. For example, periods of an enhanced biogeochemical sink would reduce the downstream advection of alkalinity and hence increase the net advective input of alkalinity to the region.

The nonnitrogenous alkalinity budget does not differ greatly from the total alkalinity budget; the main difference is that the biogeochemical sink is increased by 2% to  $22.4 \pm 25.5 \text{ mol m}^{-3} \text{ year}^{-1}$  (Figures 8b–8c, dashed lines).

To assess possible causes of the alkalinity sink, annual and seasonal estimates of the sink ( $-J$ ) were correlated with bivalve biomass and SAV coverage (Table S6). For bivalve biomass and SAV area, the seasonal period chosen was August–October and June–October, respectively, which corresponds to months during which the annual surveys were conducted

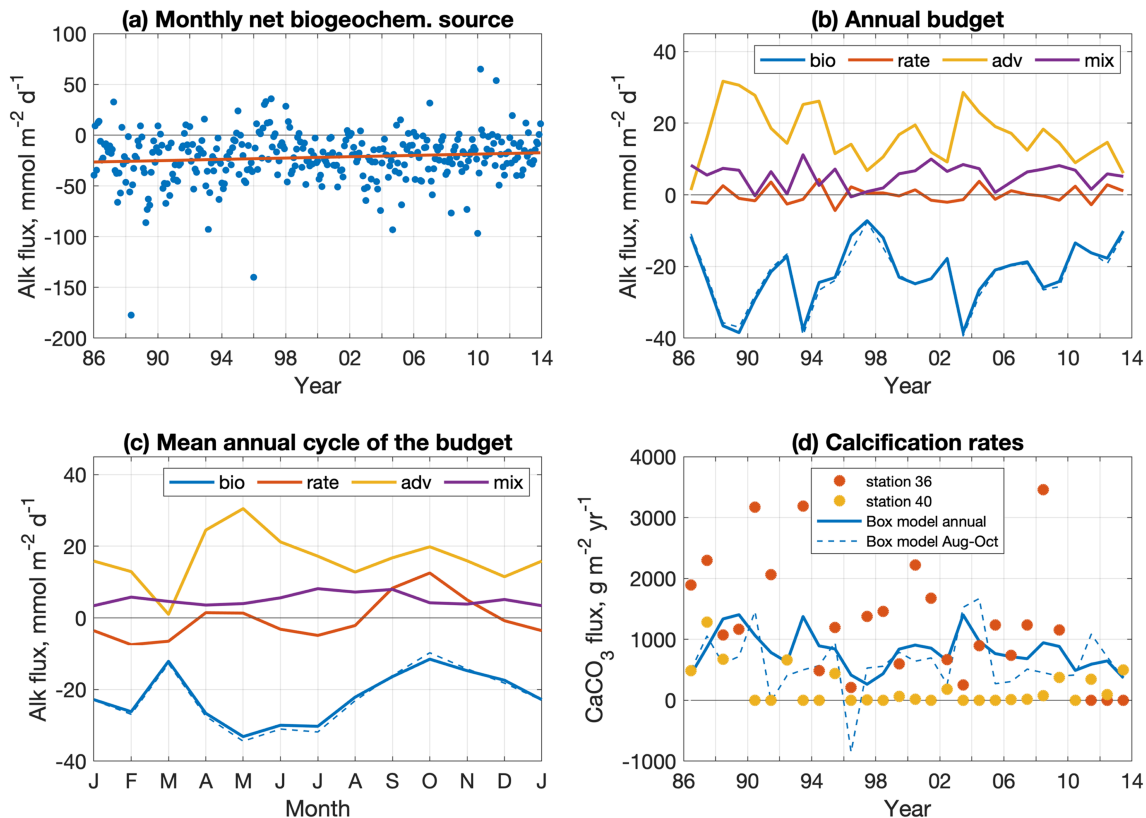


**Figure 8.** Potomac River Estuary box model results and comparison with bivalve calcification estimates. (a) Monthly estimates of the net biogeochemical source from 1986 to 2013 and a linear fit to these estimates. Annual averages (b) and mean annual cycles (c) of the individual budget terms in Equation S2 divided by the surface area of the box: bio = net biogeochemical source,  $\alpha^{-1}\bar{J}V$ ; adv = advection,  $\alpha^{-1}Q(C_R - C_D)$ ; mix = mixing,  $\alpha^{-1}K\alpha_D(\partial C/\partial x)_D$ ; and rate = time rate of change,  $\alpha^{-1}V\partial\bar{C}/\partial t$ . Dashed blue lines show net biogeochemical source of nonnitrogenous alkalinity. (d) Points show estimates of calcification rate based on bivalve biomass in the tidal fresh (station 36) and oligohaline (station 40) portions of the estuary (Figure 1). Lines show annual (solid) and August–October (dashed) calcification rate inferred from the box model.

**Table 5***Alkalinity-Salinity Relationships From the Current and Prior Research and Implied Alkalinity Trends ( $\Delta A/\Delta t$ ) at Salinities  $S$  of 0 and 10*

Tidal tributary	Earlier work		This work <sup>d</sup>		$\Delta A/\Delta t$ (mmol m <sup>-3</sup> year <sup>-1</sup> )	
	$A = (\text{mmol m}^{-3})$	Years	$A = (\text{mmol m}^{-3})$	Years	$S = 0$	$S = 10$
Susquehanna	$54.9S + 447^a$	1959–1960	$43.3S + 794$	1986–1991	12	8.0
Patuxent	$53.2S + 558^b$	1939	$46.1S + 740$	1986–1990	3.7	2.2
James	$58.0S + 407^c$	1977	$37.9S + 889$	1992–1999	22	12

*Note.* The trend for  $S = 0$  is the trend of the apparent zero-salinity endmember and not necessarily that of the nontidal river.

<sup>a</sup>The slope and intercept are the average slope and intercept from 24 monthly fits made by Carpenter et al. (1975) in the upper mainstem Chesapeake Bay. The standard deviation of the slope and intercept are 2.1 and 77 mmol m<sup>-3</sup>, respectively. <sup>b</sup>Based on 16 measurements made by Brust and Newcombe (1940) across salinities of 8 to 21 and depths of 1 to 35 m.  $R^2$  of the fit is 0.96. <sup>c</sup>Based on a linear fit to alkalinity data of Wong (1979) for salinities of 10, 15, and 20: 1000, 1250, and 1580 mmol m<sup>-3</sup>. <sup>d</sup>Fits are to the data in Figures 3b, 3c, and 3g.

(supporting information Text S4). All but one of the correlations were found to have less than 95% confidence. The one correlation exceeding 95% confidence was between Box 1 (tidal fresh) bivalve biomass and the annual sink ( $r = 0.41$ ,  $p = 0.04$ ).

Although the correlations between the alkalinity sink and bivalve biomass are weak, the estimated magnitude of the bivalve alkalinity sink based on the model of Chauvaud et al. (2003) is substantial. Figure 8d shows that the box-model estimate of August–October calcification rate falls between the bivalve calcification rate estimates at the tidal fresh and oligohaline stations. The mean  $\pm 1$  standard deviation ( $n = 28$ ) calcification rate implied by the box model is  $802 \pm 312$  g CaCO<sub>3</sub> m<sup>-2</sup> year<sup>-1</sup> for the whole year and  $609 \pm 489$  g CaCO<sub>3</sub> m<sup>-2</sup> year<sup>-1</sup> for the August–October period, whereas the averages for the upstream and downstream stations (August–October) are  $1249 \pm 996$  and  $194 \pm 311$  g CaCO<sub>3</sub> m<sup>-2</sup> year<sup>-1</sup>, respectively.

The fixed station bivalve biomass data in the tidal fresh region (station 36, Figures 1b and S1a) do not appear to be biased in any systematic way when compared with random station data (described in supporting information Text S4). Correlation exceeding 95% confidence was present between biomass at the fixed and random stations ( $r = 0.66$ ,  $p < 0.01$ ), with a slope of nearly 1. The means over the period of overlap (1995–2013) were also similar at 33.4 and 32.7 g m<sup>-2</sup> for the fixed and random sampling, respectively. The distributions of the data differed, however, with the medians of the fixed station and the random stations being 29.7 and 1.9 g m<sup>-2</sup>, respectively; the random station data are skewed low compared to the fixed station data. In contrast to the tidal fresh region, the fixed station bivalve biomass data in the oligohaline region (station 40, Figures 1b and S1b) do not appear to be well represented by the fixed station in that region. The correlation between fixed and random data is negative and the medians differ dramatically: 0.7 g m<sup>-2</sup> for the fixed station and 0.005 g m<sup>-2</sup> for the random stations, again indicating that the random station data are skewed low with respect to the fixed station data.

## 4. Discussion

### 4.1. Comparison With Other Alkalinity Studies in the Chesapeake Bay

Early studies of alkalinity in Chesapeake Bay were focused on the Patuxent (Brust & Newcombe, 1940), Susquehanna (Carpenter et al., 1975), and James (Wong, 1979) River Estuaries while more recent studies were focused on the mainstem bay (Brodeur et al., 2019; Cai et al., 2017). These studies all showed strong, positive alkalinity-salinity relationships, and generally revealed greater variability in alkalinity at low salinity compared to high salinity. Table 5 compares such relationships with those derived from fits to data for the corresponding tidal tributaries in Figure 3. Compared to the earlier fits, the more recent ones have lower slopes and higher intercepts, which is consistent with alkalinity at zero salinity increasing with time and an unchanging alkalinity at high salinity. The implied trends in alkalinity at zero salinity are substantial and can be compared to observed riverine trends: 7.0 and 15 mmol m<sup>-3</sup> year<sup>-1</sup> for the Susquehanna and Patuxent Rivers, respectively (1978–2010, Kaushal et al., 2013) and 1.9 mmol m<sup>-3</sup> year<sup>-1</sup> for the James River (1977–1996, this work). Although river and estuarine trends are all positive, direct comparisons between the river trends and the intercept trends are hampered by the different analysis time periods, at least for the Susquehanna and Patuxent systems. Furthermore, the fits based on data from the early studies are



limited to mesohaline salinities, at least for the Patuxent and James River Estuaries (salinities were not provided in Carpenter et al., 1975), in which the alkalinity at zero salinity was estimated by extrapolation of the linear fit to the mesohaline data. This means that the trends more likely represent the trends of the apparent zero-salinity endmember, which can vary as a result of changes in internal sources and sinks, as we suggested for stations in the Potomac and Chester River Estuaries (section 3.4). It can be stated more confidently that alkalinity in the mesohaline portions of the Susquehanna, Patuxent, and James River Estuaries has increased. It also seems likely that increases in river alkalinity have at least contributed to the estuarine alkalinity increases.

Prasad et al. (2013) analyzed Chesapeake Bay Program alkalinity data from 1985 to 2005 at 11 stations in the Anacostia River and 4 stations in the Potomac River Estuary. Increasing trends with  $p < 0.05$  were noted, but we are unable to compare with their results because rates were not provided. Furthermore, we were not able to locate alkalinity data in the Chesapeake Bay Program data base for the two most downstream stations presented in Prasad et al. (2013), LE2.2 and LE2.3.

#### 4.2. Alkalinity Sink Estimates in the Potomac River Estuary

There are now three sources of estimates for the alkalinity sink in the upper Potomac River Estuary: the process-based model of Cerco et al. (2013), the apparent zero-salinity endmember approach (section 3.5.1), and a box model (section 3.5.2). Cerco et al. (2013) reported results for June–August 1994, 1996, and 1999 for the tidal fresh Potomac River Estuary, which has a surface area of  $1.54 \times 10^8 \text{ m}^2$ , less than half the surface area of the box model. These 3 years were chosen to contrast average, wet, and dry hydrological conditions, respectively. The alkalinity sink was found to be 36.3, 21.0, and 43.9  $\text{mmol m}^{-2} \text{ day}^{-1}$ , respectively, and was due to the net effects of algal uptake of ammonium and nitrate, nitrification, and  $\text{CaCO}_3$  deposition (see equation (4) in Cerco et al., 2013). Box model estimates for these three time periods are 23.0, 4.9, and 23.5  $\text{mmol m}^{-2} \text{ day}^{-1}$ , respectively. The agreement is fairly good in June–August 1994 and 1999 despite the fact that the domains are rather different. In June–August 1996, the box model estimate is much lower than that of Cerco et al. (2013). Both Cerco et al. (2013) and the box model indicate that the alkalinity sink increases as streamflow decreases.

There is reasonable agreement between the alkalinity sinks estimated by the box model and the AZE approaches. A direct comparison is facilitated by identical time periods for the two models (1986–2013) and similar domains, with the surface area of the AZE model domain only 14% less than that of the box model. The mean box model sink ( $\pm 1$  standard error of the mean of the monthly fluxes) is  $21.9 \pm 1.3 \text{ mmol m}^{-2} \text{ day}^{-1}$  and is much closer to the AZE model sink based on the effective long-term mean alkalinity ( $20 \pm 2 \text{ mmol m}^{-2} \text{ day}^{-1}$ ) than the sink based on the actual mean river alkalinity and ( $48 \pm 2 \text{ mmol m}^{-2} \text{ day}^{-1}$ ). The box model is the more robust of the two approaches, given that it has far fewer assumptions. The comparison suggests that the AZE approach produces more robust results when used with long-term data and an effective long-term mean river alkalinity. Regnier et al. (1998) have also suggested that the AZE approach be used with care.

#### 4.3. Ecological Influences on Estuarine Alkalinity

We analyzed the relationship between SAV area and the alkalinity sink in the Potomac River Estuary because recent work has considered the potential of seagrasses to impact particulate inorganic carbon pools. In addition to creating habitat for benthic calcifying organisms, Hendriks et al. (2014) reported a relationship between the ambient carbonate system and calcium carbonate content of seagrass leaves. Mazarrasa et al. (2015) assessed global inorganic carbon deposition in seagrass ecosystems by comparing absence/presence data sets and found higher values in tropical and subtropical seagrass meadows with linear declines associated with latitude. There has been less work on SAV in low-salinity waters. Brodeur et al. (2019) suggested a relationship between SAV and inorganic carbon removal measured in the Susquehanna Flats, a low-salinity deltaic region of the upper Chesapeake Bay characterized by large SAV meadows. However, the mechanism for this uptake in the form of benthic, calcifying organisms found within meadows versus epiphytes or leaf content is unknown.

The results we report showing no significant relationship with SAV may point to a more nuanced dynamic between habitat and inorganic carbon. Bivalve populations have fluctuated in the Potomac River Estuary, with large increases associated with the nonnative Asiatic clam, *Corbicula fluminea* (Cohen et al., 1984;



**Table 6**

Summary of Estuarine Alkalinity Studies, Indicating Whether Alkalinity Was Thought to Behave Conservatively, be Produced (Source), or be Consumed (Sink)

Estuary	Source, sink, or conservative	Reference
<i>Chesapeake Bay</i>		
Whole	Sink, $-12 \text{ mmol m}^{-2} \text{ day}^{-1}$	Waldbusser et al. (2013)
Mainstem (upper)	Conservative	Carpenter et al. (1975)
Mainstem	Source (sulfate reduction, deep central) and sink (upper)	Cai et al. (2017)
Mainstem	Source and sink, $-1.7$ to $5.0$ (mean $0.7$ ) $\text{mmol m}^{-2} \text{ day}^{-1}$ (a)	Brodeur et al. (2019)
Mainstem	Sink, $-10 \pm 6 \text{ mmol m}^{-2} \text{ day}^{-1}$ (upper)	This study
Patuxent River	Conservative	Brust and Newcombe (1940)
Patuxent River	Sink, $-11 \pm 3 \text{ mmol m}^{-2} \text{ day}^{-1}$	This study
Potomac River	Sink, variety of processes, $-36 \text{ mmol m}^{-2} \text{ day}^{-1}$	Cerco et al. (2013)
Potomac River	Sink, $-22 \pm 1 \text{ mmol m}^{-2} \text{ day}^{-1}$	This study
Rappahannock River	Source, $5 \pm 3 \text{ mmol m}^{-2} \text{ day}^{-1}$	This study
York-Pamunkey River	Source, sulfate reduction, $8 \text{ mmol m}^{-2} \text{ day}^{-1}$	Raymond et al. (2000)
York-Mattaponi River	Source, $15 \pm 5 \text{ mmol m}^{-2} \text{ day}^{-1}$	This study
York-Pamunkey River	Source, $12 \pm 5 \text{ mmol m}^{-2} \text{ day}^{-1}$	This study
James River	Conservative or sink	Wong (1979)
James River	Sink, $-5 \pm 3 \text{ mmol m}^{-2} \text{ day}^{-1}$	This study
<i>Other North America</i>		
St. Lawrence River, Canada	Conservative	Pelletier and Lebel (1979)
Altamaha River, US	Source, $18 \text{ mmol m}^{-2} \text{ day}^{-1}$	Cai and Wang (1998)
Columbia River, US	Conservative	Park et al. (1971)
Delaware Bay, US	Conservative	Cifuentes et al. (1990)
Delaware Bay, US	Source, $3.4 \text{ mmol m}^{-2} \text{ day}^{-1}$	Joesoef et al. (2017)
Duplin River, US	Source, $30 \text{ mmol m}^{-2} \text{ day}^{-1}$	Wang and Cai (2004)
Fraser River, US	Sink	De Mora (1983)
Long Island Sound, US	Conservative	Turekian (1971)
Northwestern Gulf of Mexico coastal bays, US	Sink	Hu et al. (2015)
San Francisco Bay, US	Conservative	Cifuentes et al. (1990)
Tomas Bay, US	Source (sulfate reduction), $15 \text{ mmol m}^{-2} \text{ day}^{-1}$	Smith and Hollibaugh (1997)
<i>Europe</i>		
Skive Fjord, Denmark	Source and sink	Carstensen et al. (2018)
Ringkøbing Fjord, Denmark	Source and sink	Carstensen et al. (2018)
Roskilde Fjord, Denmark	Source and sink	Carstensen et al. (2018)
Gironde Estuary, France	Source, denitrification, and $\text{CaCO}_3$ dissolution	Abril et al. (1999)
Elbe River, Germany	Source	Kempe (1982)
Ems River, Netherlands	Source	Kempe (1982)
Scheldt, Netherlands	Conservative	Mook and Koene (1975)
Scheldt, Netherlands	Source and sink, ammonium, and nitrate cycling	Frankignoulle et al. (1996)
Scheldt, Netherlands	Source and sink, nitrate, and ammonium variations	Abril and Frankignoulle (2001)
Western Wadden Sea, Netherlands	Source, sink, or conservative	Hoppema (1990)
Framvaren Fjord, Norway	Source (sulfate reduction)	Yao and Millero (1995)
Tweed River, UK	Conservative	Howland et al. (2000)
<i>Asia</i>		
Pearl River, China	Sink	Dai et al. (2006)
Yellow River, China	Sink	Liu et al. (2014)

Note. Rates are given where available. a = Averages over the mainstem Bay. Range is in monthly values. Original units were  $10^9 \text{ mol mon}^{-1}$  or  $10^9 \text{ mol year}^{-1}$ . Converted to  $\text{mmol m}^{-2} \text{ day}^{-1}$  using an area of  $5.85 \times 10^9 \text{ m}^2$ , which was computed by summing the areas of Segments 1–8 in Chesapeake Bay Program (2004).

Phelps, 1994; this study). *Corbicula* do not require SAV habitat, but there is evidence that high filtration rates can contribute to a light environment that encourages SAV expansion, thereby creating a feedback associating SAV with bivalve abundance (e.g., Newell & Koch, 2004). Phelps (1994) proposed this mechanism as an explanation for the coupled changes in SAV coverage and *Corbicula* biomass in the Potomac River Estuary below Washington D.C. from the late 1980s through the 1990s. However, benthic organisms are also susceptible to changes in recruitment, top-down grazing, and extremes in temperature, especially freezing events (e.g., Castañeda et al., 2018; Leuven et al., 2014) that are periodic in the tidal fresh portion of the Potomac River Estuary. Given these factors, it is not surprising that abundance of bivalves is more explanatory than SAV coverage; while there may be positive feedbacks between SAV and bivalve

populations, extreme impacts to the bivalve populations are likely due to factors that do not impact the vegetation, such as freezing winter temperatures outside of the growing season.

Alkalinity is changing in many riverine systems and, as has been shown here, is influencing the alkalinity of estuaries. However, the biological implications of changing riverine alkalinity are unknown. The analysis presented here of seven tidal tributaries of the Chesapeake Bay suggests that sinks are more likely when the rivers feeding the tidal tributary are high in alkalinity and that sources are more likely when these rivers are low in alkalinity. Thus, as alkalinity of a given river changes, one might expect the source/sink characteristics of its receiving estuary to change as well. It is thus tempting to suggest that the trend of increasing alkalinity seen in many rivers (Kaushal et al., 2013; Stets et al., 2014) will lead to increases in the sink of alkalinity in the receiving estuary. However, this does not appear to be the case for the Potomac River Estuary, whose sink is declining (Figure 8) as the alkalinity of the river increases (Table 3). Other factors must come into play, with possible candidates being changing water quality, invasive species, and climate change.

#### 4.4. Diversity and Significance of Estuarine Alkalinity Dynamics

We summarize the available studies of estuarine alkalinity in Table 6, highlighting whether alkalinity behaves conservatively, is consumed or is produced within the estuary. In Chesapeake Bay, a diversity of behavior is present across and within its tidal tributaries. Early studies suggested conservative behavior of alkalinity in the Patuxent (Brust & Newcombe, 1940) and Susquehanna (Carpenter et al., 1975) River Estuaries and the possibility of a sink in the James River Estuary (Wong, 1979). More recent studies suggest alkalinity sinks in the tidal fresh and oligohaline portions of the Susquehanna (Brodeur et al., 2019; Cai et al., 2017) and Potomac (Cerco et al., 2013) River Estuaries and sources (due to sulfate reduction) in the York River Estuary (Raymond et al., 2000), which are in broad agreement with our findings. Brodeur et al. (2019) suggested that the alkalinity sink in the upper mainstem bay was due to SAV in the Susquehanna Flats, although these authors found the mainstem bay as a whole to be a weak source on average, with significant seasonal fluctuations. Subpycnocline waters have been found to be a source due to sulfate reduction (Cai et al., 2017). The only study to address the bay as a whole is that of Waldbusser et al. (2013), who deduced the bay to be an alkalinity sink by constructing a single alkalinity-salinity relationship for the whole bay and combining it with a box model. The deduced sink is within the range of the sinks we found for individual tidal tributaries, despite the fact that their box model is based on the mainstem bay while the alkalinity data are mainly from the Potomac River Estuary.

The relationship between nontidal river alkalinity and nonconservative behavior of alkalinity in the receiving tidal tributary that was discovered for Chesapeake Bay tributaries (Figure 7) suggests a possible role of the  $\text{CaCO}_3$  saturation state in governing estuarine alkalinity dynamics. Invoking the explicit conservative form of alkalinity (equation (1)), we speculate that the calcium ion concentration and hence  $\text{CaCO}_3$  saturation index increases with alkalinity in Chesapeake Bay tributaries. The excess of calcification over dissolution would likely be enhanced as the saturation index increases, and this could explain the pattern in Figure 7. Other candidates for nonconservative behavior in Chesapeake Bay tributaries involve nitrogen and sulfur cycling. The analysis presented here suggests a small role for nitrogen in the alkalinity budget except in the Patuxent River Estuary (Table 4). Sulfur cycling, via net sulfate reduction in estuarine sediments or fringing tidal wetland soils, would serve only as an alkalinity source. Net sulfate reduction in the mainstem of Chesapeake Bay, as inferred from sulfur burial rates, ranged from  $0.51$  to  $1.1 \text{ mol S m}^{-2} \text{ year}^{-1}$  (Marvin-DiPasquale & Capone, 1998), or  $3\text{--}6 \text{ mmol m}^{-2} \text{ day}^{-1}$  of alkalinity production, which is comparable in magnitude to the nonconservative fluxes for some Chesapeake Bay tributaries (Tables 4 and 6). Hence, it seems plausible that net  $\text{CaCO}_3$  precipitation and net sulfate reduction both play roles in nonconservative alkalinity behavior in Chesapeake Bay tributaries.

Other estuaries throughout the world show a range of behavior similar to that observed in the Chesapeake Bay. Excluding the Chesapeake Bay studies, there are eight studies suggesting conservative behavior, 10 suggesting a sink, and 13 suggesting a source. There is a tendency for early studies—all six in Table 6 published before 1980—to come to the conclusion of conservative behavior. Indeed, this is not an unreasonable conclusion to draw from many alkalinity-salinity plots because the difference in freshwater and oceanic end-members is often very pronounced, overwhelming any nonconservative effects.

How important is nonconservative behavior to alkalinity and carbon budgets in estuaries? Based on the AZE approach using the effective long-term mean river alkalinity, tidal tributaries of the Chesapeake Bay may either consume as much as 27% or add as much as 172% of the riverine alkalinity input (Table 4 results using the effective mean river alkalinity). Dissolved inorganic carbon (DIC) and alkalinity are approximately equal in rivers. For example, using Stets and Striegl's (2012) DIC load and mean streamflow for the Susquehanna River, we compute an effective long-term mean DIC concentration of  $850 \text{ mol m}^{-3}$ , which is only 10% greater than this river's effective long-term mean alkalinity (Table 1). This means that a substantial fraction of the inorganic carbon input is also affected by the same processes that influence alkalinity (e.g., calcification and sulfate reduction). How about for other estuaries? According to Table 6, a typical magnitude of an estuarine alkalinity flux (either source or sink) might be roughly  $10 \text{ mmol m}^{-2} \text{ day}^{-1}$  and as high as  $40 \text{ mmol m}^{-2} \text{ day}^{-1}$ , which are equivalent to a dissolution or precipitation of calcium carbonate of 22 and  $88 \text{ g C m}^{-2} \text{ year}^{-1}$ , respectively. These are significant fluxes when compared to estimates of global-mean  $\text{CO}_2$  outgassing (Chen et al., 2013) and primary production (Cloern et al., 2014) of estuaries, which are 93 and  $252 \text{ g C m}^{-2} \text{ year}^{-1}$ , respectively. Hence, alkalinity dynamics need to be considered when constructing estuarine carbon budgets.

## 5. Conclusions

A large data set of alkalinity measurements from an estuarine system with multiple tidal tributaries has been analyzed. The main findings of this analysis are as follows:

1. There is a nearly order-of-magnitude variation of the long-term mean alkalinity among the seven main rivers draining to the Chesapeake Bay. Riverine alkalinity has a strong annual cycle and has a strong negative relationship with streamflow.
2. At high salinities, alkalinity generally increases with salinity as a result of mixing between low- and high-salinity endmembers. All of the tidal tributaries converge to a common value of alkalinity at high salinity.
3. At the 25 stations where alkalinity has been measured for two decades or more, significant long-term increasing trends are present that are in excess of the trends of the rivers draining to those stations. Changes in nitrogen cycling and an increased contribution of high-salinity, high-alkalinity water are also ruled out, leaving changes in other nonconservative processes (e.g., declines in  $\text{CaCO}_3$  precipitation) the likely cause of the trends. Comparison with earlier and later alkalinity measurements also suggests that alkalinity in Chesapeake Bay has been rising.
4. There are alkalinity sinks in the Susquehanna, Patuxent, James, and Potomac River Estuaries that remove between 8% and 27% of the riverine alkalinity input. In contrast, the Rappahannock, Mattaponi, and Pamunkey River Estuaries have sources of alkalinity amounting to 34% to 171% of the river input. The fraction of the riverine alkalinity input that is biogeochemically removed in the tidal tributary shows a tendency to increase with riverine alkalinity. The sink in the Potomac River Estuary has declined by more than half from 1986 to 2013. The magnitude of the sink is consistent with a simple model of calcification, mainly by the bivalve *Corbicula fluminea*.

The Chesapeake Bay's tidal tributaries reflect the diversity of alkalinity behavior among the world's estuaries, with some systems acting as alkalinity sources, some as alkalinity sinks, and some close to neutral. This diversity of behavior is probably due to the wide range of lithologies that characterize the watersheds of the Chesapeake Bay, which leads to the wide range of riverine alkalinity among the tidal tributaries. From a quantitative perspective, the Chesapeake Bay also seems representative in that the estimated sources and sinks are comparable to other systems around the world.

Sources and sinks of alkalinity not only affect the speciation of carbonic acid and its dissociation products but also add and remove carbon at rates that are comparable to other important carbon cycle processes in estuaries, such as  $\text{CO}_2$  outgassing. Hence, alkalinity dynamics should be considered when studying the carbon balance of an estuary.

From a historical perspective, alkalinity, along with pH, is one of the more commonly measured carbonate system parameters in estuaries. Our analysis reveals what can be learned about estuarine carbon cycling from long-term water quality monitoring programs, which have been traditionally focused more on

nutrients and water clarity. It is likely that there are many monitoring programs with long-term alkalinity data sets that still have much to teach us.

### Acknowledgments

This research was supported with funding from the National Science Foundation's Chemical Oceanography Program (OCE-1536996 and OCE-1537013) and Research Experiences for Undergraduates (REU) Program (AGS-1560339, Penn State REU in Climate Science, supporting S. Cintrón Del Valle). Additional support was provided by NASA through Grants NNX14AM37G and NNX14AF93G. We are grateful to Rob Ceres for helpful discussions early in this study. This is VIMS Manuscript 3860 and UMCES Manuscript 5723. Data used in this study are archived at The Pennsylvania State University's institutional repository, ScholarSphere (Najjar et al., 2019).

### References

- Abril, G., Etcheber, H., Le Hir, P., Bassoullet, P., Boutier, B., & Frankignoulle, M. (1999). Oxic/anoxic oscillations and organic carbon mineralization in an estuarine maximum turbidity zone (The Gironde, France). *Limnology and Oceanography*, 44(5), 1304–1315. <https://doi.org/10.4319/lo.1999.44.5.1304>
- Abril, G., & Frankignoulle, M. (2001). Nitrogen–alkalinity interactions in the highly polluted Scheldt basin (Belgium). *Water Research*, 35(3), 844–850. [https://doi.org/10.1016/S0043-1354\(00\)00310-9](https://doi.org/10.1016/S0043-1354(00)00310-9)
- Bates, N. R., & Hansell, D. A. (1999). A high resolution study of surface layer hydrographic and biogeochemical properties between Chesapeake Bay and Bermuda. *Marine Chemistry*, 67(1–2), 1–16. [https://doi.org/10.1016/S0304-4203\(99\)00045-6](https://doi.org/10.1016/S0304-4203(99)00045-6)
- Boyle, E., Collier, R., Dengler, A. T., Edmond, J. M., Ng, A. C., & Stallard, R. F. (1974). On the chemical mass-balance in estuaries. *Geochimica et Cosmochimica Acta*, 38(11), 1719–1728. [https://doi.org/10.1016/0016-7037\(74\)90188-4](https://doi.org/10.1016/0016-7037(74)90188-4)
- Brewer, P. G., Wong, G. T. F., Bacon, M. P., & Spencer, D. W. (1975). An oceanic calcium problem? *Earth and Planetary Science Letters*, 26(1), 81–87. [https://doi.org/10.1016/0012-821X\(75\)90179-X](https://doi.org/10.1016/0012-821X(75)90179-X)
- Bricker, S. B., Rice, K. C., & Bricker, O. P. III (2014). From headwaters to coast: Influence of human activities on water quality of the Potomac River Estuary. *Aquatic Geochemistry*, 20(2–3), 291–323. <https://doi.org/10.1007/s10498-014-9226-y>
- Brodeur, J. R., Chen, B., Su, J., Xu, Y. Y., Hussain, N., Scaboo, K. M., et al. (2019). Chesapeake Bay inorganic carbon: Spatial distribution and seasonal variability. *Frontiers in Marine Science*, 6, 99. <https://doi.org/10.3389/fmars.2019.00099>
- Brust, H. F., & Newcombe, C. L. (1940). Observations on the alkalinity of estuarine waters of the Chesapeake Bay near Solomons Island, Maryland. *Journal of Marine Research*, 3, 105–111.
- Cai, W.-J., Hu, X., Huang, W. J., Murrell, M. C., Lehrter, J. C., Lohrenz, S. E., et al. (2011). Acidification of subsurface coastal waters enhanced by eutrophication. *Nature Geoscience*, 4(11), 766–770. <https://doi.org/10.1038/NNGEO1297>
- Cai, W.-J., Huang, W. J., Luther, G. W., Pierrot, D., Li, M., Testa, J., et al. (2017). Redox reactions and weak buffering capacity lead to acidification in the Chesapeake Bay. *Nature Communications*, 8(1), 369. <https://doi.org/10.1038/s41467-017-00417-7>
- Cai, W.-J., & Wang, Y. (1998). The chemistry, fluxes, and sources of carbon dioxide in the estuarine waters of the Satilla and Altamaha Rivers, Georgia. *Limnology and Oceanography*, 43, 657–668. <https://doi.org/10.4319/lo.1998.43.4.0657>
- Carpenter, J., Bradford, W., & Grant, V. (1975). Processes affecting the composition of estuarine waters (HCO<sub>3</sub>, Fe, Mn, Zn, Cu, Ni, Cr, Co, and Cd). In L. E. Cronin (Ed.), *Estuarine Research, Volume 1: Chemistry, Biology, and the Estuarine System*, (Vol. 1, pp. 188–214). New York, NY: Academic Press.
- Carstensen, J., Chierici, M., Gustafsson, B. G., & Gustafsson, E. (2018). Long-term and seasonal trends in estuarine and coastal carbonate systems. *Global Biogeochemical Cycles*, 32, 497–513. <https://doi.org/10.1002/2017GB005781>
- Carstensen, J., & Duarte, C. M. (2019). Drivers of pH variability in coastal ecosystems. *Environmental Science & Technology*, 53(8), 4020–4029. <https://doi.org/10.1021/acs.est.8b03655>
- Castañeda, R. A., Cvetanovska, E., Hamelin, K. M., Simard, M. A., & Ricciardi, A. (2018). Distribution, abundance and condition of an invasive bivalve (*Corbicula fluminea*) along an artificial thermal gradient in the St. Lawrence River. *Aquatic Invasions*, 13, 379–392. <https://doi.org/10.3391/ai.2018.13.3.06>
- Cerco, C. F., Threadgill, T., Noel, M. R., & Hinz, S. (2013). Modeling the pH in the tidal fresh Potomac River under conditions of varying hydrology and loads. *Ecological Modelling*, 257, 101–112. <https://doi.org/10.1016/j.ecolmodel.2013.02.011>
- Chauvaud, L., Thompson, J. K., Cloern, J. E., & Thouzeau, G. (2003). Clams as CO<sub>2</sub> generators: The *Potamocorbula amurensis* example in San Francisco Bay. *Limnology and Oceanography*, 48(6), 2086–2092. <https://doi.org/10.4319/lo.2003.48.6.2086>
- Chen, C.-T., Huang, T.-H., Chen, Y.-C., Bai, Y., He, X., & Kang, Y. (2013). Air–sea exchanges of CO<sub>2</sub> in the world's coastal seas. *Biogeosciences*, 10(10), 6509–6544. <https://doi.org/10.5194/bg-10-6509-2013>
- Chesapeake Bay Program. (2004). Chesapeake Bay Program analytical segmentation scheme: Revisions, decisions and rationales, 1983–2003. Annapolis, Maryland.
- Cifuentes, L. A., Schemel, L. E., & Sharp, J. H. (1990). Qualitative and numerical analyses of the effects of river inflow variations on mixing diagrams in estuaries. *Estuarine, Coastal and Shelf Science*, 30(4), 411–427. [https://doi.org/10.1016/0272-7714\(90\)90006-D](https://doi.org/10.1016/0272-7714(90)90006-D)
- Cloern, J. E., Foster, S. Q., & Kleckner, A. E. (2014). Phytoplankton primary production in the world's estuarine-coastal ecosystems. *Biogeosciences*, 11(9), 2477–2501. <https://doi.org/10.5194/bg-11-2477-2014>
- Cohen, R. R. H., Dresler, P. V., Phillips, E. J. P., & Cory, R. L. (1984). The effect of the Asiatic clam, *Corbicula fluminea*, on phytoplankton of the Potomac River, Maryland. *Limnology and Oceanography*, 29(1), 170–180. <https://doi.org/10.4319/lo.1984.29.1.0170>
- Dai, M., Guo, X., Zhai, W., Yuan, L., Wang, B., Wang, L., et al. (2006). Oxygen depletion in the upper reach of the Pearl River estuary during a winter drought. *Marine Chemistry*, 102(1–2), 159–169. <https://doi.org/10.1016/j.marchem.2005.09.020>
- De Mora, S. J. (1983). The distribution of alkalinity and pH in the Fraser Estuary. *Environmental Technology*, 4(1), 35–46.
- Dickson, A. G. (1981). An exact definition of total alkalinity and a procedure for the estimation of alkalinity and total inorganic carbon from titration data. *Deep-Sea Research*, 26, 609–623.
- Drake, T. W., Tank, S. E., Zhulidov, A. V., Holmes, R. M., Gurtovaya, T., & Spencer, R. G. (2018). Increasing alkalinity export from large Russian Arctic rivers. *Environmental Science & Technology*, 52(15), 8302–8308. <https://doi.org/10.1021/acs.est.8b01051>
- Frankignoulle, M., Bourge, I., & Wollast, R. (1996). Atmospheric CO<sub>2</sub> fluxes in a highly polluted estuary (the Scheldt). *Limnology and Oceanography*, 41(2), 365–369. <https://doi.org/10.4319/lo.1996.41.2.0365>
- Godsey, S. E., Kirchner, J. W., & Clow, D. W. (2009). Concentration–discharge relationships reflect chemostatic characteristics of US catchments. *Hydrological Processes*, 23(13), 1844–1864. <https://doi.org/10.1002/hyp.7315>
- Gustafsson, E., Hagens, M., Sun, X., Reed, D. C., Humborg, C., Slomp, C. P., & Gustafsson, B. G. (2019). Sedimentary alkalinity generation and long-term alkalinity development in the Baltic Sea. *Biogeosciences*, 16(2), 437–456. <https://doi.org/10.5194/bg-16-437-2019>
- Hendriks, I. E., Olsen, Y. S., Ramajo, L., Basso, L., Moore, T. S., Howard, J., & Duarte, C. M. (2014). Photosynthetic activity buffers ocean acidification in seagrass meadows. *Biogeosciences*, 11, 333–346. <https://doi.org/10.5194/bg-11-333-2014>
- Hirsch, R. M., Moyer, D. L., & Archfield, S. A. (2010). Weighted Regressions on Time, Discharge, and Season (WRTDS), with an application to Chesapeake Bay river inputs. *Journal of the American Water Resources Association*, 46(5), 857–880. <https://doi.org/10.1111/j.1752-1688.2010.00482.x>



- Hoppema, J. M. J. (1990). The distribution and seasonal variation of alkalinity in the Southern Bight of the North Sea and in the Western Wadden Sea. *Netherlands Journal of Sea Research*, 26(1), 11–23. [https://doi.org/10.1016/0077-7579\(90\)90053-J](https://doi.org/10.1016/0077-7579(90)90053-J)
- Howland, R. J. M., Tappin, A. D., Uncles, R. J., Plummer, D. H., & Bloomer, N. J. (2000). Distributions and seasonal variability of pH and alkalinity in the Tweed Estuary, UK. *Science of The Total Environment*, 251–252, 125–138. [https://doi.org/10.1016/S0048-9697\(00\)00406-X](https://doi.org/10.1016/S0048-9697(00)00406-X)
- Hu, X., Beseres Pollack, J., McCutcheon, M. R., Montagna, P. A., & Ouyang, Z. (2015). Long-term alkalinity decrease and acidification of estuaries in Northwestern Gulf of Mexico. *Environmental Science & Technology*, 49(6), 3401–3409. <https://doi.org/10.1021/es505945p>
- Joeseof, A., Kirchman, D. L., Sommerfield, C. K., & Cai, W.-J. (2017). Seasonal variability of the inorganic carbon system in a large coastal plain estuary. *Biogeosciences*, 14, 4949–4963. <https://doi.org/10.5194/bg-14-4949-2017>
- Karrh, R., Domotor, D., Golden, R., Karrh, L., Landry, B., Romano, W., et al. (2013). *Potomac river water and habitat quality assessment*. Annapolis, MD: Maryland Department of Natural Resources.
- Kempe, S. (1982). Valdivia cruise, October 1981: Carbonate equilibria in the estuaries of Elbe, Weser, Ems and in the southern German Bight. In E. T. Degens (Ed.), *Transport of Carbon and Minerals in Major World Rivers, Part 1 (Volume 1, SCOPE/UNEP special issue 52) (pp. 719–742)*: Mitt. Geol. Palaont. Inst. Univ. Hamburg.
- Kaushal, S. S., Likens, G. E., Utz, R. M., Pace, M. L., Grese, M., & Yepsen, M. (2013). Increased river alkalization in the Eastern U.S. *Environmental Science & Technology*, 47(18), 10302–10311. <https://doi.org/10.1021/es401046s>
- Leuven, R. S., Collas, F. P., Koopman, K. R., Matthews, J., & Velde, G. (2014). Mass mortality of invasive zebra and quagga mussels by desiccation during severe winter conditions. *Aquatic Invasions*, 9, 243–252. <https://doi.org/10.3391/ai.2014.9.3.02>
- Liu, Z., Zhang, L., Cai, W.-J., Wang, L., Xue, M., & Zhang, X. (2014). Removal of dissolved inorganic carbon in the Yellow River Estuary. *Limnology and Oceanography*, 59(2), 413–426. <https://doi.org/10.4319/lo.2014.59.2.0413>
- Loder, T. C., & Reichard, R. P. (1981). The dynamics of conservative mixing in estuaries. *Estuaries and Coasts*, 4(1), 64–69. <https://doi.org/10.2307/1351543>
- Manickam, S., Barbaroux, L., & Ottmann, F. (1985). Composition and mineralogy of suspended sediment in the fluvio-estuarine zone of the Loire River, France. *Sedimentology*, 32(5), 721–741. <https://doi.org/10.1111/j.1365-3091.1985.tb00484.x>
- Marvin-DiPasquale, M. C., & Capone, D. G. (1998). Benthic sulfate reduction along the Chesapeake Bay central channel. I. Spatial trends and controls. *Marine Ecology Progress Series*, 168, 213–228. <https://doi.org/10.3354/meps168213>
- Mazarrasa, I., Marbà, N., Lovelock, C. E., Serrano, O., Lavery, P. S., Fourqurean, J. W., et al. (2015). Seagrass meadows as a globally significant carbonate reservoir. *Biogeosciences*, 12(16), 4993–5003. <https://doi.org/10.5194/bg-12-4993-2015>
- Mook, W. G., & Koene, B. K. S. (1975). Chemistry of dissolved inorganic carbon in estuarine and coastal brackish waters. *Estuarine and Coastal Marine Science*, 3(3), 325–336. [https://doi.org/10.1016/0302-3524\(75\)90032-8](https://doi.org/10.1016/0302-3524(75)90032-8)
- Müller, J. D., Schneider, B., & Rehder, G. (2016). Long-term alkalinity trends in the Baltic Sea and their implications for CO<sub>2</sub>-induced acidification. *Limnology and Oceanography*, 61(6), 1984–2002. <https://doi.org/10.1002/lno.10349>
- Najjar, R. G., Herrmann, M., Cintrón Del Valle, S. M., Friedman, J. R., Friedrichs, M. A. M., Harris, L. A., et al. (2019). Dataset for “Alkalinity in Tidal Tributaries of the Chesapeake Bay”. Dataset. <https://doi.org/10.26207/w1vs-jz06>
- Newell, R. I., & Koch, E. W. (2004). Modeling seagrass density and distribution in response to changes in turbidity stemming from bivalve filtration and seagrass sediment stabilization. *Estuaries*, 27(5), 793–806. <https://doi.org/10.1007/BF02912041>
- Officer, C. B. (1980). Box models revisited. In P. Hamilton, & K. B. Macdonald (Eds.), *Estuarine and wetland processes: With emphasis on modeling*, (pp. 65–114). Boston, MA: Springer US.
- Orth, R. J., Wilcox, D. J., Whiting, J. R., Kenne, A. K., & Smith, E. R. (2018). Section: 01 Line Frame: 01 Aug27-17: Aerial Imagery Acquired to Monitor the Distribution and Abundance of Submerged Aquatic Vegetation in Chesapeake Bay and Coastal Bays. <https://scholarworks.wm.edu/data/156>.
- Park, P. K., Osterberg, C. L., & Forster, W. O. (1971). Chemical budget of The Columbia River. In A. T. Pruter, & D. L. Alverson (Eds.), *The Columbia River Estuary and Adjacent Ocean Waters*, (pp. 123–134). Seattle and London: University of Washington Press.
- Pelletier, E., & Lebel, J. (1979). Hydrochemistry of dissolved inorganic carbon in the St. Lawrence Estuary (Canada). *Estuarine and Coastal Marine Science*, 9(6), 785–795. [https://doi.org/10.1016/S0302-3524\(79\)80011-0](https://doi.org/10.1016/S0302-3524(79)80011-0)
- Phelps, H. L. (1994). The Asiatic clam (*Corbicula fluminea*) invasion and system-level ecological change in the Potomac River estuary near Washington, DC. *Estuaries*, 17(3), 614–621. <https://doi.org/10.2307/1352409>
- Prasad, M. B. K., Kaushal, S. S., & Murtugudde, R. (2013). Long-term pCO<sub>2</sub> dynamics in rivers in the Chesapeake Bay watershed. *Applied Geochemistry*, 31, 209–215. <https://doi.org/10.1016/j.apgeochem.2013.01.006>
- Raymond, P. A., Bauer, J. E., & Cole, J. J. (2000). Atmospheric CO<sub>2</sub> evasion, dissolved inorganic carbon production, and net heterotrophy in the York River estuary. *Limnology and Oceanography*, 45, 1707–1717. <https://doi.org/10.4319/lo.2000.45.8.1707>
- Raymond, P. A., & Oh, N.-H. (2009). Long term changes of chemical weathering products in rivers heavily impacted from acid mine drainage: Insights on the impact of coal mining on regional and global carbon and sulfur budgets. *Earth and Planetary Science Letters*, 284(1), 50–56. <https://doi.org/10.1016/j.epsl.2009.04.006>
- Raymond, P. A., Oh, N.-H., Turner, R. E., & Broussard, W. (2008). Anthropogenically enhanced fluxes of water and carbon from the Mississippi River. *Nature*, 451(7177), 449–452. <https://doi.org/10.1038/nature06505>
- Regnier, P., Mouchet, A., Wollast, R., & Rondon, F. (1998). A discussion of methods for estimating residual fluxes in strong tidal estuaries. *Continental Shelf Research*, 18(13), 1543–1571. [https://doi.org/10.1016/S0278-4343\(98\)00071-5](https://doi.org/10.1016/S0278-4343(98)00071-5)
- Shadwick, E. H., Friedrichs, M. A. M., Najjar, R. G., De Meo, O. A., Friedman, J. R., Da, F., & Reay, W. G. (2019). High-frequency CO<sub>2</sub> system variability over the winter-to-spring transition in a coastal plain estuary. *Journal of Geophysical Research: Oceans*, 124, 7626–7642. <https://doi.org/10.1029/2019JC015246>
- Shen, C., Testa, J. M., Li, M., Cai, W. J., Waldbusser, G. G., Ni, W., et al. (2019). Controls on carbonate system dynamics in a coastal plain estuary: A modeling study. *Journal of Geophysical Research: Biogeosciences*, 124, 61–78. <https://doi.org/10.1029/2018JG004802>
- Smith, S. V., & Hollibaugh, J. T. (1997). Annual cycle and interannual variability of ecosystem metabolism in a temperate climate embayment. *Ecological Monographs*, 67, 509–533. [https://doi.org/10.1890/0012-9615\(1997\)067\[0509:ACAIVO\]2.0.CO;2](https://doi.org/10.1890/0012-9615(1997)067[0509:ACAIVO]2.0.CO;2)
- Stets, E. G., Kelly, V. J., & Crawford, C. G. (2014). Long-term trends in alkalinity in large rivers of the conterminous US in relation to acidification, agriculture, and hydrologic modification. *Science of the Total Environment*, 488–489, 280–289. <https://doi.org/10.1016/j.scitotenv.2014.04.054>
- Stets, E. G., & Striegl, R. G. (2012). Carbon export by rivers draining the conterminous United States. *Inland Waters*, 2(4), 177–184. <https://doi.org/10.5268/IW-2.4.510>
- Tian, R. (2019). Factors controlling saltwater intrusion across multi-time scales in estuaries, Chester River, Chesapeake Bay. *Estuarine, Coastal and Shelf Science*, 223, 61–73. <https://doi.org/10.1016/j.ecss.2019.04.041>

- Turekian, K. K. (1971). 2. Rivers, tributaries, and estuaries. In D. W. Hood (Ed.), *Impingement of man on the oceans*, (pp. 9–73). New York: Wiley–Interscience.
- Waldbusser, G. G., Powell, E. N., & Mann, R. (2013). Ecosystem effects of shell aggregations and cycling in coastal waters: An example of Chesapeake Bay oyster reefs. *Ecology*, 94(4), 895–903. <https://doi.org/10.1890/12-1179.1>
- Wang, Z. A., & Cai, W. J. (2004). Carbon dioxide degassing and inorganic carbon export from a marsh-dominated estuary (the Duplin River): A marsh CO<sub>2</sub> pump. *Limnology and Oceanography*, 49, 341–354.
- Wartel, S., & Faas, R. W. (1986). Calcium carbonate in Schelde-estuary bottom sediments. *Bull. Inst. r. Sci. nat. Belg.: Sciences de la Terre*, 56, 383–390.
- Wolf-Gladrow, D. A., Zeebe, R. E., Klaas, C., Körtzinger, A., & Dickson, A. G. (2007). Total alkalinity: The explicit conservative expression and its application to biogeochemical processes. *Marine Chemistry*, 106(1), 287–300. <https://doi.org/10.1016/j.marchem.2007.01.006>
- Wong, G. T. F. (1979). Alkalinity and pH in the southern Chesapeake Bay and the James River estuary. *Limnology and Oceanography*, 24(5), 970–977. <https://doi.org/10.4319/lo.1979.24.5.0970>
- Yao, W., & Millero, F. J. (1995). The chemistry of the anoxic waters in the Framvaren Fjord, Norway. *Aquatic Geochemistry*, 1(1), 53–88. <https://doi.org/10.1007/BF01025231>

## References From the Supporting Information

- Austin, J. A. (2004). Estimating effective longitudinal dispersion in the Chesapeake Bay. *Estuarine, Coastal and Shelf Science*, 60, 359–368. <https://doi.org/10.1016/j.ecss.2004.01.012>
- Chesapeake Bay Program (1996). *Recommended guidelines for sampling and analyses in the Chesapeake Bay Monitoring Program*: U. S. Environmental Protection Agency.
- Chesapeake Bay Program (2012). *Guide to using Chesapeake Bay Program water quality monitoring data*. Annapolis, MD: Chesapeake Bay Program.
- ESRI (2011). *ArcGIS Desktop: Release 10*. Redlands, CA: Environmental Systems Research Institute.
- Llansó, R. J., & Zaveta, D. (2017). *Chesapeake Bay water quality monitoring program long-term benthic monitoring and assessment component Level 1 comprehensive report July 1984–December 2016 (Volume 1)*. Columbia, MD: Versar, Inc.
- McMahon, R. F. (2002). Evolutionary and physiological adaptations of aquatic invasive animals: *r* selection versus resistance. *Canadian Journal of Fisheries and Aquatic Sciences*, 59(7), 1235–1244. <https://doi.org/10.1139/f02-105>
- Moyer, D. L., & Blomquist, J. D. (2018). Nitrogen, phosphorus, and suspended-sediment loads and trends measured at the Chesapeake Bay River input monitoring stations: Water years 1985–2017, U.S. Geological Survey Data Release. <https://doi.org/10.5066/P96NUK3Q>
- National Geophysical Data Center. (1999). U.S. coastal relief model–Southeast Atlantic: National Oceanographic and Atmospheric Administration.
- Strickland, J. D. H., & Parsons, T. R. (1972). *A practical handbook of seawater analysis*, (Second ed.). Ottawa, Canada: Fisheries Research Board of Canada.